แบบจำลองบัลลิสติกดิพอซิชันที่มีการแพร่บนผิวสำหรับการปลูกฟิล์มบางบนซับสเตรตที่มีแบบรูป

นายชลาศรัย ไชยศร

วิทยานิพนธ์นี้เป็นส่วนหนึ่งของการศึกษาตามหลักสูตรปริญญาวิทยาศาสตรมหาบัณฑิต
สาขาวิชาฟิสิกส์ ภาควิชาฟิสิกส์
คณะวิทยาศาสตร์ จุฬาลงกรณ์มหาวิทยาลัย
ปีการศึกษา ๒๕๕๐

BALLISTIC DEPOSITION MODEL WITH SURFACE DIFFUSION FOR THIN FILM GROWTH ON PATTERNED SUBSTRATES

Mr. Chalasai Chaiyasorn

A Thesis Submitted in Partial Fulfillment of the Requirements
for the Degree of Master of Science Program in Physics
Department of Physics
Faculty of Science
Chulalongkorn University
Academic year 2007

Thesis Title	BALLISTIC DEPOSITION MODEL WITH SURFACE DIFFUSION FOR THIN FILM GROWH ON PATTERNED SUBSTRATES
By	Mr. Chalasai Chaiyasorn
Field of Study	Physics
Thesis Advisor	Assistant Professor Patcha Chatraphorn, Ph.D.

Accepted by the Faculty of Science, Chulalongkorn University in Partial Fulfillment of the Requirements for the Master's Degree

..... Dean of the Faculty of Science

(Professor Supot Hannongbua, Ph.D.)

THESIS COMMITTEE

..... Chairman

(Associate Professor Mayuree Natenapit, Ph.D.)

..... Thesis Advisor

(Assistant Professor Patcha Chatraphorn, Ph.D.)

..... Member

(Assistant Professor Nakorn Phaisangittisakul, Ph.D.)

..... Member

(Chatchai Srinitiwarawong, Ph.D.)

ชลาศรัย ไชยศร : แบบจำลองบัลลิสติกดิพอซิชันที่มีการแพร่บนผิวสำหรับการปลูกฟิล์มบางบนซับสเตรตที่มีแบบรูป (BALLISTIC DEPOSITION MODEL WITH SURFACE DIFFUSION FOR THIN FILM GROWTH ON PATTERNED SUBSTRATES) อาจารย์ที่ปรึกษา : ผศ. ดร. ปัจฉา ฉัตราภรณ์, ๖๘ หน้า

แบบจำลองบัลลิสติกดิพอซิชันเป็นแบบจำลองทางคอมพิวเตอร์อย่างง่ายประเภทหนึ่งที่ใช้สำหรับอธิบายการปลูกฟิล์มบางที่มีตำหนิประเภทช่องว่าง เพื่อที่จะให้แบบจำลองสมจริงมากขึ้นจึงได้มีการต่อเติมกระบวนการแพร่บนผิวเข้ามายังแบบจำลอง ในงานนี้การตีความที่แตกต่างกันของกระบวนการแพร่บนผิวส่งผลให้เกิดแบบจำลองที่แตกต่างกันสองแบบ คือ แบบจำลองมาตรฐานที่ใช้กันเป็นส่วนใหญ่ และแบบจำลองที่ใกล้เคียงกับความเป็นจริง เพื่อแสดงให้เห็นความแตกต่างระหว่างแบบจำลองทั้งสองนี้จึงได้ทำการศึกษาสัณฐานของฟิล์ม ความขรุขระของพื้นผิวฟิล์ม และความหนาแน่นของตำหนิประเภทช่องว่างภายในเนื้อฟิล์ม ผลจากการจำลองพบว่าฟิล์มที่ปลูกจากแบบจำลองทั้งสองมีพื้นผิวที่เรียบมากขึ้นพร้อมกับมีความหนาแน่นของตำหนิประเภทช่องว่างภายในฟิล์มลดลงเมื่อมีการเพิ่มอุณหภูมิของซับสเตรต แต่อย่างไรก็ตามอุณหภูมิของซับสเตรตที่สูงทำให้เกิดการแกว่งของกราฟที่ใช้บอกระดับความขรุขระของพื้นผิวฟิล์มในกรณีของแบบจำลองมาตรฐาน ในขณะที่กราฟของแบบจำลองที่ใกล้เคียงกับความเป็นจริงนั้นยังคงรักษาความสัมพันธ์ที่เป็นไปตามกฎของเลขยกกำลังไปกับเวลาที่ใช้ในการปลูกฟิล์ม ในการศึกษาการปลูกฟิล์มลงบนซับสเตรตที่มีแบบรูปเราได้ใช้แบบจำลองที่ใกล้เคียงกับความเป็นจริง โดยทำการศึกษาบนซับสเตรตสองชนิด ได้แก่ ซับสเตรตที่เรียบ และซับสเตรตที่มีแบบรูป ค่าความน่าจะเป็นของการคงอยู่เป็นปริมาณที่บอกว่าแบบรูปของซับสเตรตถูกรักษาเอาไว้ได้มากน้อยเพียงใดหลังจากกระบวนการปลูกฟิล์มเสร็จสิ้นลง ซึ่งเราพบว่าค่าความน่าจะเป็นของการคงอยู่ของฟิล์มที่ปลูกลงบนซับสเตรตทั้งสองชนิดลดลงไปกับเวลาที่ใช้ในการปลูกฟิล์ม ถ้าเวลาคงที่ อุณหภูมิของซับสเตรตเป็นปัจจัยสำคัญในการควบคุมแบบรูปของฟิล์ม เราพบว่ามีเพียงช่วงอุณหภูมิแคบๆ เท่านั้นที่ฟิล์มสามารถรักษาแบบรูปเดิมเอาไว้ได้นานที่สุด และเรายังพบว่าถ้าส่วนที่เรียบของซับสเตรตกว้างขึ้นแบบรูปเดิมก็สามารถคงอยู่ได้นานขึ้น

ภาควิชา ฟิสิกส์ ลายมือชื่อนิสิต ชลาศรัย ไชยศร

สาขาวิชา ฟิสิกส์ ลายมือชื่ออาจารย์ที่ปรึกษา ปัจฉา ฉัตราภรณ์

ปีการศึกษา ๒๕๕๐

4772263323 : MAJOR PHYSICS
KEY WORDS : BALLISTIC DEPOSITION MODEL/ SURFACE DIFFUSION/ PATTERNED SUBSTRATE/ PERSISTENCE PROBABILITY

CHALASAI CHAIYASORN : BALLISTIC DEPOSITION MODEL WITH SURFACE DIFFUSION FOR THIN FILM GROWTH ON PATTERNED SUBSTRATES. THESIS ADVISOR : ASST. PROF. PATCHA CHATRAPHORN, PH.D., 68 pp.

Ballistic deposition model is a simple computational model described the growth of thin film with void defect. To make it more realistic, a surface diffusion process is added into the model. In this work, different interpretations of this process result in two different models, a "conventional" model and a "realistic" model. To see the difference between these models, the film's morphology, interface width and defect density are studied. Simulation results show that the films from both models have smoother surfaces with less void defect density when the substrate temperature is increased. However, high substrate temperature leads to oscillations of the interface width curve in the conventional model while the curve of the realistic model maintains a power law relation with growth time. When studying the growth on patterned substrates, the realistic model was used. Two types of substrate, a flat substrate and a periodic patterned substrate, were studied. Persistence probability is a quantity that provides information on how much the pattern of the substrate is kept after the growth process is complete. Here, we found that the persistence probabilities of the films grown on both substrates decrease with the growth time. If the time is fixed, the substrate temperature plays an important role in controlling the film's pattern. We found that there is only a narrow window of temperature that the film can maintain its original pattern longest. Also, we found that if the flat part of the substrate is larger, the original pattern of the film can survive longer.

Department of Physics
Field of study Physics
Academic year 2007

Student's signature Chalasai Chaiyasorn
Advisor's signature Patcha Chatraphorn

Acknowledgements

After a long time, my thesis is finally completed. Here, I would like to express my sincere gratitude to Asst. Prof. Dr. Patcha Chatraphorn for a chance to work in this field. Thanks for all her suggestions and encouragement for creating the best work. I would like to thank Asst. Prof. Dr. Sojiphong Chatraphorn for the facilities on high efficiency computer and a well organized work station. His prompt response to any problems in the station is highly appreciated. Furthermore, I would like to thank Asst. Prof. Dr. Nattakorn Tubthong for his suggestion on programming. He always frees to answer all questions regarding my program and also to debug my complicated code. I would like to thank Asst. Prof. Dr. Sukkaneste Tungasmita for his idea about the surface diffusion process that allows all surface particles to diffuse at a time. This idea not only increases the thickness of my thesis, it also makes my work even more worthwhile.

I would like to thank Assoc. Prof. Dr. Mayuree Natenapit, Asst. Prof. Dr. Nakorn Pisarngittisakul, and Dr. Chatchat Srinitiwarawong for the time from their busy schedules to be my thesis committee. Their comments on this thesis are also greatly appreciated.

Thanks to Sitthidate Nanure for his advice on data structure and algorithm. They helped me save a lot of simulation time and also make the idea of Dr. Sukkaneste comes true. Thanks to all the staffs at my research unit and all my friends for every comment and idea. These make my work more complete.

Thanks to all my family's members who always provide me money, love, and encouragement to reach my goal. Without them, it is very difficult for me to be on this day. Thanks to everyone who have walked into my life. All experiences I have gained challenge me to meet a new one. Finally, thanks to you the reader who has picked my thesis. I hope that my work can meet your requirement.

This thesis is partially supported by the Office of Commission for Higher Education-CU Graduate Thesis Grant, Graduate School, Chulalongkorn University.

Table of Contents

List of Tables

List of Figures

Figure Page

Chapter 1
Introduction

Ballistic deposition (BD) model is a numerical model created by Vold in 1959 for the formation of sedimentary rocks [1]. In 1966, Sutherland modified the model to make it more complete [2]. Since then, this model has become a well-known model widely used in many other simulations such as the growth of porous media [3-5], the adhesion of red blood cells on a collector [6], and the evolution of thin films with void defect [7-10]. The only process simulated in this model is the deposition process. Although the conditions designed for the BD model are quite simple, they are enough to describe very low temperature vapor deposition thin film growth systems effectively. This was confirmed from experimental films that yield similar results with the BD films [11-15]. For this reason, the BD model is usually selected to be a based model for studying many additional factors [16-19], including the substrate temperature [20-21]. In experiments, the substrate temperature is increased to reduce the void defect and to smooth the film surface [22-23]. However, physical processes actually occurred on the film during growth are still not completely understood. To study this, in 1994, Das Sarma et al. [20] added a surface diffusion process into the BD model. In the surface diffusion process, surface particles can diffuse continuously on the film with the diffusion rate that depends on the substrate temperature and the coordination number of the diffusing particles. By using this modified model, they found that [20] the change of simulated films agrees well with that of the experimental films.

Nowadays, the growth on patterned substrates plays an important role in creating many atomic scale devices, e.g. quantum dots [24-27], quantum wires [28-31], devices for Micro-Electro-Mechanical Systems (MEMS) [32-35] and resonators of organic semiconductor lasers [36-39]. The crucial factor for these innovations is that the film should maintain its original structure throughout the growth process. However, this is quite difficult if the suitable conditions for the growth are not known. To understand this, computational models have been used [40, 41]. Initially, most research works concentrated on the effect of substrate temperature. Solid-on-solid models, which are models that do not allow overhang, void defect and desorption,

were used [40-41] for this problem. Nevertheless, both the overhang and the void defect are unavoidable problems in the growth at low temperature. They were expected to have a large impact in maintaining the film's pattern especially when the film is grown on a patterned substrate. In this work, the ballistic deposition model with surface diffusion was selected to study the growth of films on substrates with predetermined structures. Flat structure and periodic structure were studied. The film's morphology and persistence probability were considered in order to see how much the film can keep its original pattern at a specific time.

While using the model of Das Sarma et al. [20], it was found that the number of particles that is allowed to diffuse when the diffusion time arrives has not yet been specified. Therefore, two different interpretations of the surface diffusion process were proposed here. The first interpretation is a "conventional" model [20-21, 42-47] which allows only one surface particle to diffuse at a time, and the second interpretation is a "realistic" model that allows diffusion of *all* surface particles. To see how much this difference affects the growing film, their simulated results were characterized. Morphology, interface width and defect density were the quantities of interest.

This thesis is organized as follows. Chapter 2 provides background knowledge and related theory about thin film growth simulation and its characterization techniques. Results from our simulations together with the discussions are shown in Chapter 3. Although the different interpretation of the surface diffusion process is not the main goal of our study, its effect is also explored in both the growth on flat substrates and the growth on periodic patterned substrates. In Chapter 4, which is the final chapter of this work, the whole thesis will be concluded.

Chapter 2
Theoretical Aspects

In vapor deposition thin film growth, there are three principal processes that occurred during the growth [48]. The first process is the *deposition process*. In this process, a particle from a source is thermally evaporated and randomly moves to create a film on the substrate. If the deposited particle has energy that is high enough to break the bond(s) it has formed with its nearest-neighbor particle(s), it can travel on the film surface. This "traveling" is called the *surface diffusion process*. In the case that the energy of the deposited particle is very high, the particles can be evaporated from the film. It is called the *desorption process*. Since the type of particles in each system is fixed throughout the growth, the associated parameters (e.g. the size of particles and their binding energy) controlling the system energy are constant except the system temperature [48]. In practice, this temperature is usually convected to the film via the substrate. This means that adjusting the substrate temperature leads to varying of the energy of the system [48]. Typically, this temperature is limited within the range that the rate of the desorption process is very small in order to maintain the film particles on the substrate. Thus, there are only two significant processes left: the deposition process and the surface diffusion process. In order to understand these processes, the BD model with surface diffusion is used in this work. In this chapter, the original BD model will be introduced first. Then the surface diffusion process is added to the original model. After that, the characterization techniques for the films created from these models will be discussed.

2.1 BD model

The BD model [1-2, 8] is an epitaxy model that describes vapor deposition of low temperature particles. These particles are assumed to be unit square lattices as shown in figure 2.1. In this model, a particle is released from a source located over the substrate at a randomly chosen column. The newly released particle drops vertically along the trajectory until it reaches the film. The particle is incorporated as a part of the film when it either reaches the top of the film surface (as atom A in figure 2.1) or

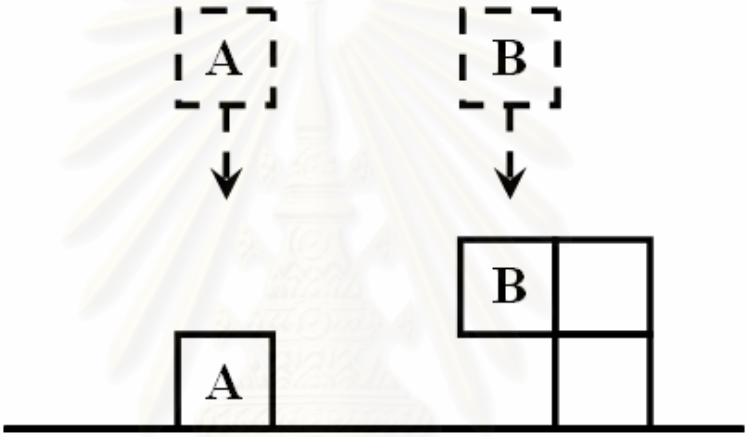

Figure 2.1: A schematic diagram described the rules of the BD model

comes into contact with a side of a nearest-neighbor column (as atom B in figure 2.1). After the incorporation, the next particle is then dropped. The latter incorporation condition, sticking to the side of an existing column, can cause vacancies, also known as void defect, in the growing film.

In programming, a periodic boundary condition is used to eliminate the edge effect. Also, it should be mentioned here that the period of a random generator used in the simulation must be large enough for the growth of each film. If the period of a random generator is not long enough, it will cause the growth in anomaly mode [49-50]. In order to prevent this problem, we use ran2 [51] as the random generator in our work.

2.2 BD Model with surface diffusion

When a surface diffusion process is added in to the model, the deposited particles are allowed to diffuse continuously on the film surface. Diffusion rate of each particle is calculated by the Arrhenius expression [20-21, 42],

$$R = R_0 exp\left(-E_n / k_B T\right), \tag{1}$$

where $R_0 = dk_BT/h$ is the characteristic vibrational frequency, d is the dimension of the substrate (d = 1 in this work), k_B is the Boltzmann constant, T is the substrate temperature and h is the Plank constant. $E_n = E_0 + nE_b$ is the activation energy that depends on the coordination number n of the diffusing particle. E_0 is the ground state energy and E_b is the binding energy per bond of the particle. In this work, these two energies are constant. They are set to be E_0 = 1.0 eV and E_b = 0.3 eV [20-21, 48], which are the energy of silicon (Si) [20-21, 48]. From equation (1) we can see that the diffusion rate R depends on the substrate temperature T and the coordination number n. Table 2.1 shows the values of R for various T and n. It is clear from table 2.1 that if T is fixed, as it is in each simulation, R decreases quickly when n increases. For the same value of n, when T increases, R also increases. If the diffusion rate R is high enough, the surface particle can break its initial bond(s) and move to an unoccupied site nearby where it can form at least one bond. Since a desorption (evaporation) process is forbidden in this model, surface particles that may cause disconnection of a

Table 2.1: Diffusion rates of the surface particle which is a function of the nearest neighbor interaction and the temperature of the substrate

T (K)	$R_{n=1}$ (s^{-1})	$R_{n=2}$ (s^{-1})	$R_{n=3}$ (s^{-1})
500	8.20×10^{-1}	7.76×10^{-4}	7.34×10^{-7}
550	14.0	2.50×10^{-2}	4.45×10^{-5}
600	1.50×10^{2}	4.54×10^{-1}	1.37×10^{-3}
650	1.13×10^{3}	5.32	2.51×10^{-2}
700	6.37×10^{3}	44.0	3.05×10^{-1}
750	2.87×10^{4}	2.77×10^{2}	2.67
800	1.08×10^{5}	1.39×10^{3}	17.9

particle or a group of particles from the film are considered immobile. Particles with n = 4 are also not allowed to diffuse as they are not on the surface of the film. Examples of these stationary particles are illustrated in figure 2.2.

In the diffusion process, the "conventional" model [20-21, 42-47] allows only one particle to diffuse on the film at a time. That particle is selected by random from a group of particles having the highest diffusion rate (i.e. the particles with the smallest number of bonds). On the other hand, we propose a more "realistic" model that allows diffusion of all eligible particles. When these particles with the highest R diffuse, the growth time is hold until the last particle in this group completes its diffusion. To see how much this difference in the diffusion procedure affects the growing film, the simulated films from these models were characterized.

2.3 Quantities of interest

In order to understand the microscopic processes of the growing film in detail, morphology, interface width, defect density, and persistence probability are quantities that we analyzed.

2.3.1 Morphology

In general, the film morphology is the first quantity that is usually observed. For films that are grown under the solid-on-solid conditions, the morphology is only the surface of the film. It is the contour that links the highest particles in each column of the film on the substrate. However, for the BD films, the area under the surface should also be investigated. This is because the distribution of voids in the film sometimes gives some useful information. So, the morphology of these films with voids is the plot of all occupied sites on the substrate.

2.3.2 Interface width

To study how the morphology of the growing film changes in time, a statistical quantity is employed. It is the time evolution of the surface roughness or the *interface width* [48] of the film. Its definition is the root mean square height fluctuation of the film surface:

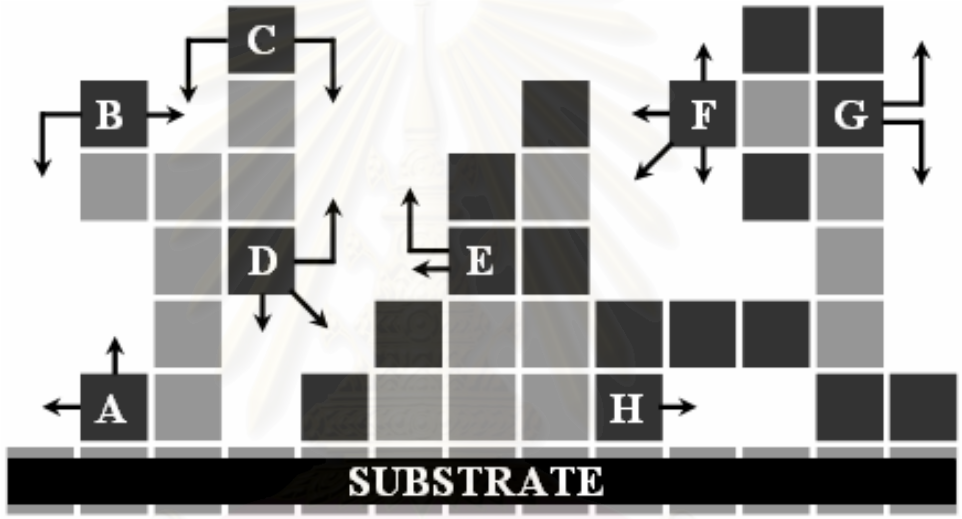

Figure 2.2: The light color blocks represent stationary particles while the dark color blocks are all eligible to diffuse. The arrows on each labeled dark block point to positions where the particle can diffuse to.

$$W(L,t) \equiv \sqrt{\left\langle \left(H(x,t) - \langle H(x,t) \rangle_L \right)^2 \right\rangle_L}, \quad (2)$$

where $H(x,t)$ is the height of column x at time t, and the rectangular brackets $<\ldots>_L$ represent the average over the substrate of size L. The interface width increases with the growth time (t) with a power law relation [48]

$$W(L,t) \sim t^{\beta}. \quad (3)$$

Here β is the *growth exponent* indicating how fast the roughness increases in time. Typically, for the growth on small substrates, the correlation between the film's surfaces of neighboring columns can lead to the saturation of the interface roughness. The saturated value of the interface roughness is sometimes called *saturation width*. It is abbreviated as W_{sat}. When plotting W-t curves of many systems with various L together on the same axes, it is found that W_{sat} depends on L through [48]

$$W_{sat}(L,t) \sim L^{\alpha}. \quad (4)$$

α is the *roughness exponent* characterizing the roughness of the saturated interface. Moreover, it is found that the *crossover time* (t_x), which is the time that the width changes from the growth region to the saturation region, also depends on L via [48]

$$t_x \sim L^{z}. \quad (5)$$

z is the *dynamic exponent* identifying the saturation time of the growing film. The combination of these three relations yields [48]

$$z = \frac{\alpha}{\beta}. \quad (6)$$

This linear equation shows that when any two of the exponents are known, the third can automatically be calculated. This means that only two exponents are enough to

predict the growth behavior of the film. Since equation (6) is derived from information at the *critical point* or the point that seemingly independent parameters t and L are linked to each other (the saturation time in this case), the exponents α, β and z are called *critical exponents* [48]. One advantage of these exponents is that they are used to identify the *universality class* of the model [48].

For models that have the same set of critical exponents, they are grouped to be in the same universality class [48]. This means that all the models that are in the same universality class generate films with the same growth behavior [48]. For example, the BD model which is a discrete model that describes the growth of porous thin films has the exponents $\alpha \approx 1/2$ and $\beta \approx 1/3$ [48]. Also, an Eden model which is another discrete model that describes the growth of bacterial colonies has the same values of α and β [48]. Therefore, both the BD model and the Eden model are in the same universality class. Since this universality class is predicted by the Kardar Parisi and Zhang (KPZ) theory, it is named the KPZ universality class [48, 52].

In 1985, Family and Vicsek observed that the shapes of W-t curves are very similar for every scale of observation (for every L in this case). By employing the scaling-invariance property [48], all the curves are rescaled. Here, W of each curve is divided by L^{α} and t of the same curve is divided by $L^{\alpha/\beta}$. When plotting rescaled curves together on the same axes (the axes of (W/L^{α}) and $(t/L^{\alpha/\beta})$), it is found that adjusting values of α and β can overlap the curves to be on the same track. This brings about the *dynamic scaling relation* [48, 53]

$$W(L,t) \sim L^{\alpha} f\left(\frac{t}{L^{\alpha/\beta}}\right), \tag{7}$$

when $f(y)$ is the scaling function. ($f(y) \sim y^{\beta}$ for $y << 1$ and $f(y)$ = constant for $y >> 1$.) This relation is widely used in predicting the time evolution of the film roughness.

In many BD simulations, it has been shown that the value of β is often less than the theoretical value of the KPZ universality class when L is small [54-55]. This is due to the strong finite-size effect in the model [55]. However, when L increases, the value of β is closed to the theoretical value. In order to obtain the asymptotic value of β (β_{∞}), β versus L^{-1} are plotted and the curve is extrapolated to $L \rightarrow \infty$. Because the curve from this plot is non-linear, in 2001 Aarão Reis proposed a scaling relation [54]

$$\beta(L) \approx \beta_{\infty} + AL^{-\lambda}, \tag{8}$$

when A is a constant and λ is the correction to scaling in equation (7). The value of λ can be adjusted to a suitable value; hence, the curve will be close to linear. Here, the β-intercept shows β_{∞}. This method is also used here and more discussion on this will be presented in Chapter 3.

2.3.3 Defect density

Since the number of void defect plays an important role in characterizing the BD model, the *defect density* is another quantity that should be investigated in this work. It is the ratio of number of unoccupied sites to the total sites of the film [20],

$$defect \quad density = \frac{number \quad of \quad unoccupied \quad sites}{number \quad of \quad total \quad sites}. \tag{9}$$

The interesting information is how the defect density changes with the growth time and the substrate temperature.

2.3.4 Persistence probability

For the growth on patterned substrates, it is important to know how much the pattern of the film can persist at a specific time. This can also be observed from the film's morphology. However, different observers may have different opinions about the film's pattern or even the same observer also has different idea if the decision takes place at different time. This problem can be solved if a statistical quantity is used instead of personal judgment. In 1997, Kallabis and Wolf proposed a probability that shows the fraction of the film's pattern that propagates through time t. It is called *persistence probability* and is defined as [56]

$$P(t) \equiv \left\langle \prod_{s=1}^{t} \delta_{H(x,s),H(x,o)+s} \right\rangle_{L}, \tag{10}$$

where $H(x,s)$ is the height of the growing interface at the column x at time s, δ is the Kronecker delta function ($\delta_{i,j} = 1$ when $i = j$ and 0 otherwise), Π is a production over time s where s starts from the first layer (s = 1 ML) to the time t, and the angular brackets $<\ldots>_L$ shows the average over the whole substrate of site L.

By definition, the persistence probability of the film can be maintained only when the film surface can keep its original pattern perfectly at all-time. This is too strict because it is found that, sometimes, although the persistence probability of the film is totally eliminated, the overall outline of the initial pattern can still be seen. In experiments, it is quite impossible to create a device with the ideal pattern. Many works allow some "error" within the film. Therefore, in 2005, Piankoranee proposed a modified definition of the persistence probability [57]. It is

$$P_n(t) \equiv \left\langle \prod_{s=1}^{t} F_{\Delta H}(s) \right\rangle_L , \tag{10}$$

where

$$F_{\Delta H}(s) = \begin{cases} 1 & if \quad [H(x,0)+s] - \Delta H \le H(x,s) \le [H(x,0)+s] + \Delta H \\ 0 & otherwise. \end{cases}$$

Although the formula looks more complicated, the physical meaning of this modified probability is mostly the same as the original definition. The only difference between these equations is at the term ΔH which is the accepted error. By definition, if the film height oscillates within this accepted range, the persistence probability of the film is not affected. So, a suitable value of ΔH will make the persistence probability of the film fits well with the film's morphology.

Note here that every quantity mentioned in this section, section 2.3, is ensemble averaged. In the next chapter, all results are averaged at 100 rounds of simulation.

Chapter 3
Results and Discussions

The presentation in this chapter is grouped into two main sections. The first section concentrates on results of films that are grown on flat substrates while the second section concentrates on results of films that are grown on patterned substrates.

3.1 BD Model: Flat substrates

In this first section, films generated from the original BD model and the BD model with surface diffusion are studied. The main goal here is to investigate the model in details and to see how various factors, such as the temperature, affect the grown films. The two interpretations of surface diffusion are also compared in this section.

3.1.1 Original model

The film generated from the original BD model in this work contains a lot of voids that are distributed uniformly inside the film. The morphology of our original BD film is shown in figure 3.1. The time evolution of the interface roughness can also be seen in figure 3.1—different shades indicate different time instant which is shown in 12 MLs time interval. Note here that a unit of time is monolayer (ML) which is defined as an interval that L particles are deposited on the one-dimensional substrate of size L. In order to see the evolution of the surface morphologies more clearly, we also show just the surfaces of this film at each time instant in figure 3.2.

The interface width of the BD films was plotted as a function of the growth time in figure 3.3. From the graph, the curve can be separated into three main regions according to the slopes. In the first region ($t \leq 0.2$ ML), the growth exponent β is approximately 0.50 which is in agreement with the value of β of a discrete model without surface diffusion that allows no void (the random deposition model [48, 58]). This is understandable because during this early time, the height of the growing film is still very low so there is less chance for overhanging to occur. Hence, the film is still more or less solid, in which there is no void. This explains why the growth exponent in this region is consistent with that of the random deposition model. In the

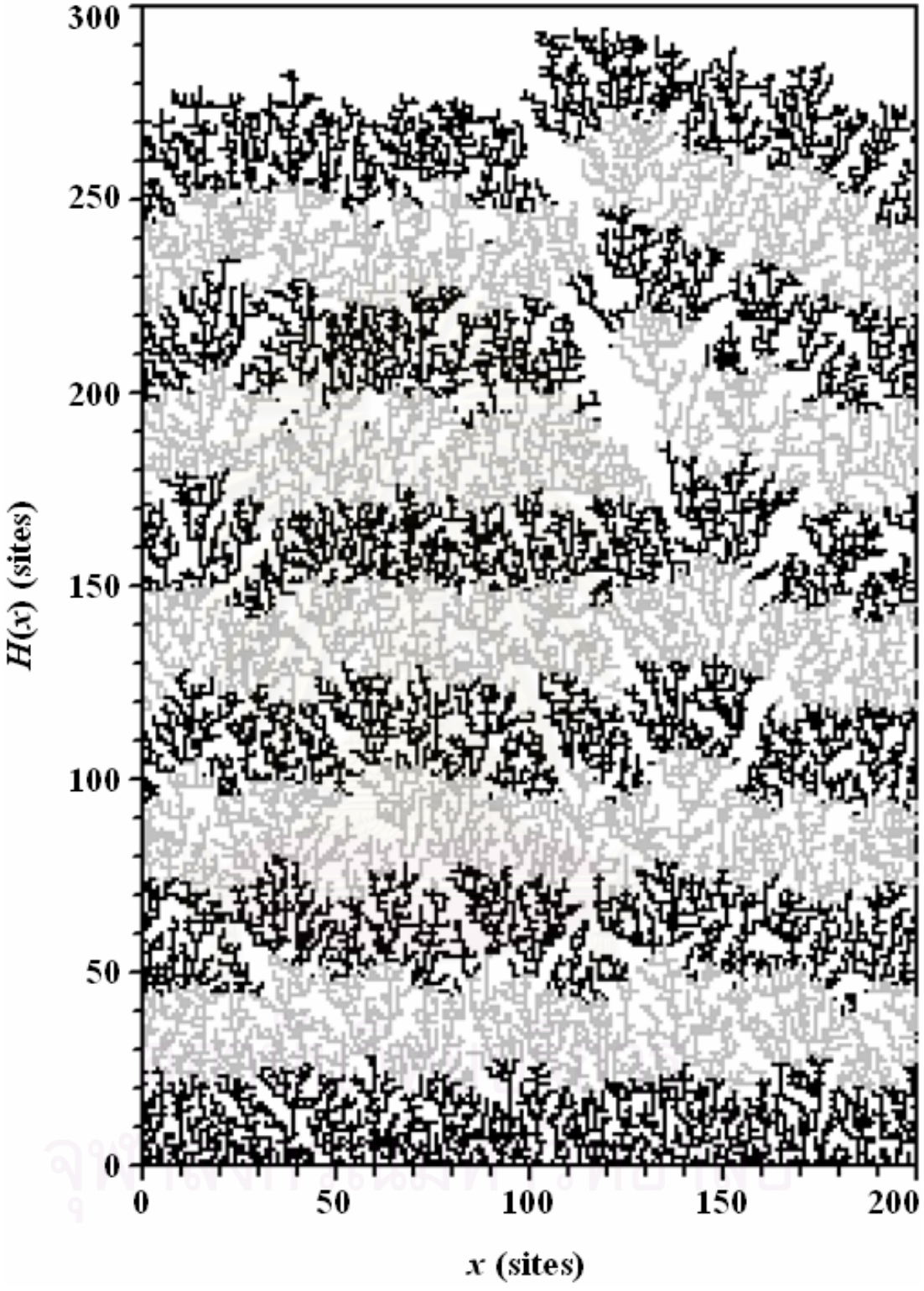

Figure 3.1: The morphology of the BD film grown on L = 200 sites when t = 132 MLs. Different shades represent different time intervals: the shading changes after every 12 MLs.

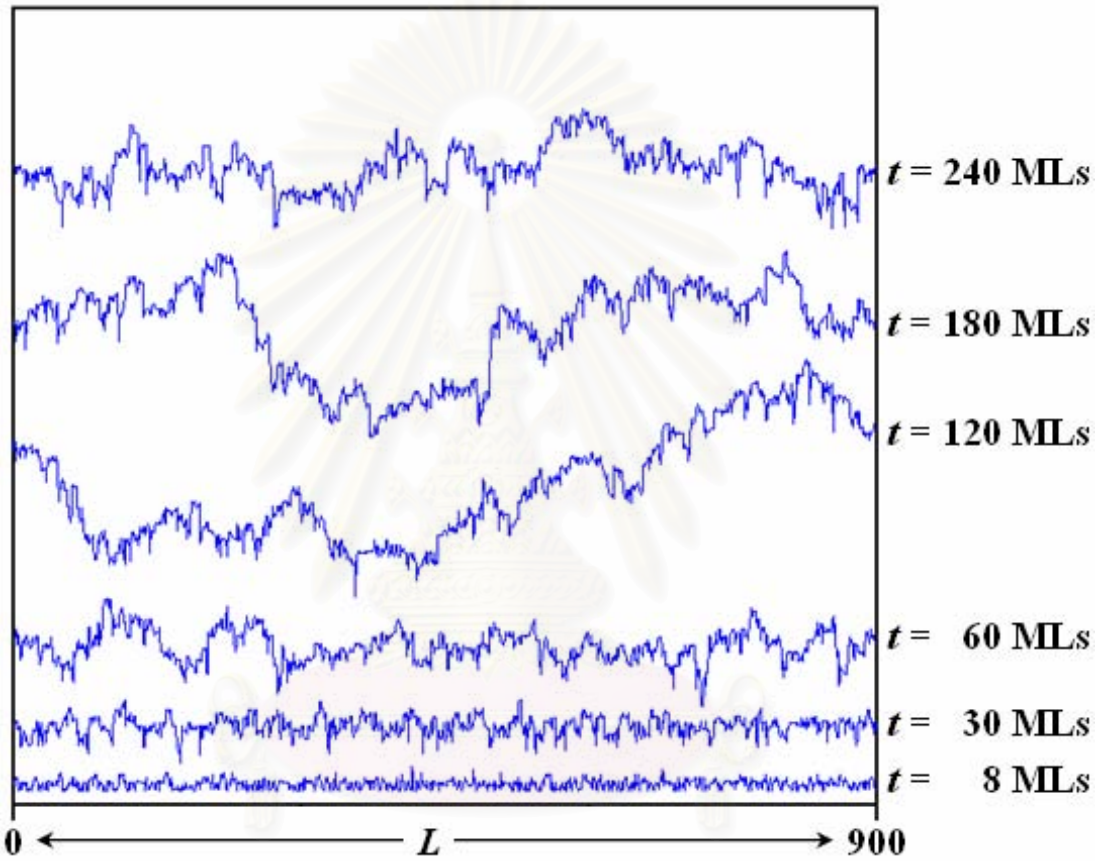

Figure 3.2: The surface morphologies of the BD film grown on L = 900 sites at different growth time

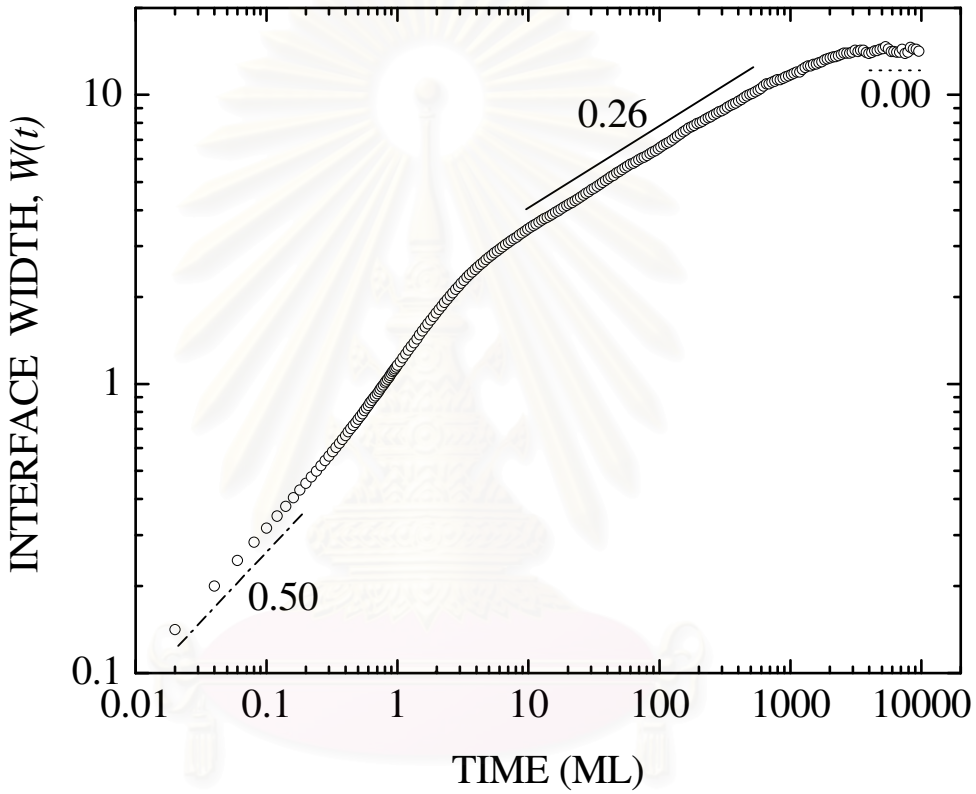

Figure 3.3: The time evolution of the interface width of the BD film that is grown on $L = 900$ sites

second region ($10 \leq t \leq 500$ MLs), the value of β falls to approximately 0.26 which is the value of β for the original BD model [54-55]. This is the region when the void defect is produced. In the last region ($t \geq 3000$ MLs), β drops to approximately zero. The roughness of the film becomes stable. This is a result of the expansion of the inter-column correlation of the film [48]. When a branch of the film which is grown from the same "root" spreads globally until it covers the entire film surface, the interface roughness of the film saturates. This is why this region is called the saturation region. The connection between each couple of regions, as known as the *crossover region*, is the region where the growth behavior of the film changes from one type to another [48]. In figure 3.3, there are two crossover regions. The first one is the change from the solid film to the film with voids while another is the change when the surface roughness of the film becomes saturated.

In figure 3.4, *W-t* curves from systems of various substrate sizes are shown on the same plot. If we take a look at figure 3.4, we see that the crossover time that the width becomes saturated depends on the size of the substrate (L). When L is small, the expansion of the branch of the film can cover the whole film surface very quickly. The saturation region can occur very fast; therefore, the saturation width is small. This can be seen from the system with L = 100 sites in figure 3.4. If L is increased, the branch of the film takes longer time to cover the whole film. The saturation region is shifted farther. As a result, the saturation width is larger. In case that L goes to infinity, the saturation region is shifted unlimited and we can no longer see it, as shown in figure 3.4 for L = 100,000 sites.

Data collapse according to relation (7) mentioned in Chapter 2 is attempted. It is found that the interface width from systems with various L in figure 3.4 can be collapsed onto one line by setting the exponents to $\alpha \approx 0.42$ and $\beta \approx 0.30$. The result is shown in the inset of the figure 3.4. These exponents which belong to the Kardar, Parisi and Zhang (KPZ) universality class are in agreement with those of the previous works [48, 52].

When investigating the slopes of the graphs in the region that $t \geq 10$ MLs, we can see that the size of the substrate directly affects the value of β of the model. This is because the smaller the values of L, the faster the crossover begins. Since the bending of the curve at the crossover region decreases the slope of the curve, β becomes smaller. Figure 3.4 shows that, at L = 100 sites, β is approximately 0.25 which is far below the theoretical value of $\beta = 1/3$ [48, 52]; in contrast, β from the

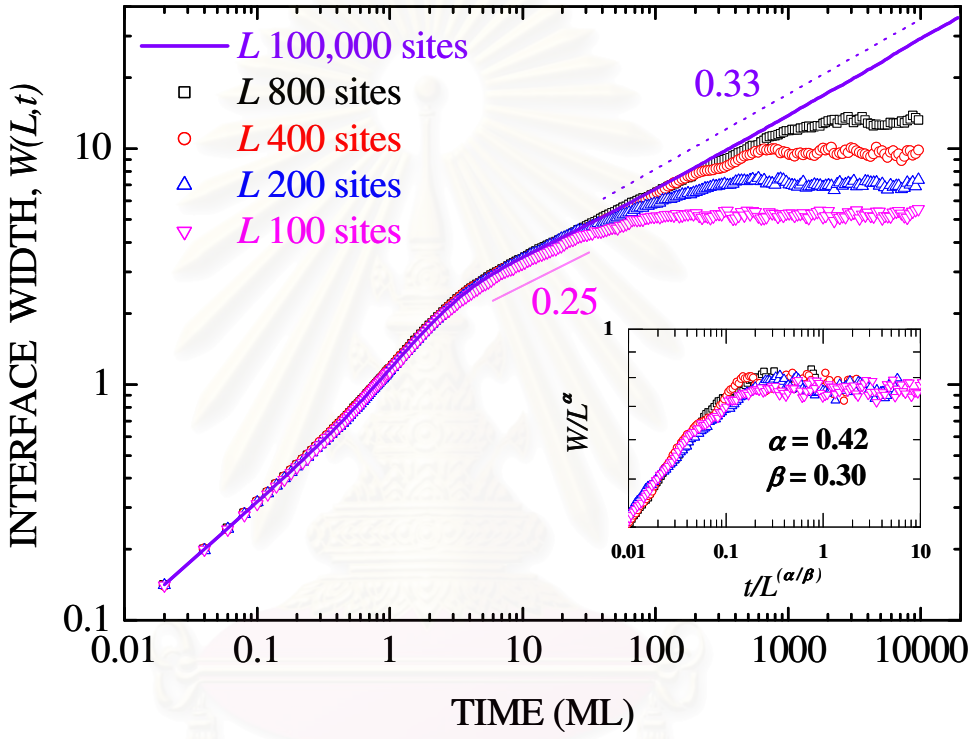

Figure 3.4: The *W-t* plots of the BD film grown on four different substrate sizes INSET: The scaling plots of the same systems

system with L = 100,000 sites represents the same value as the theory. These are also in agreement with previous works [48, 52]. In order to estimate the asymptotic value of β, we plot β from various L as a function of $L^{-\lambda}$ as discussed in Chapter 2. When λ is adjusted to be between 0.26 and 0.30, the curve is almost linear. This can be seen from the value of r^2 which is a parameter used to determine how straight the curve is. (If r^2 = 1, the curve is perfectly straight.) Here, the extrapolated value of β (β_∞ in relation (8) in Chapter 2) is closely the same as the theoretical value. This result is similar to the result of Aarão Reis [54]. Figure 3.5 shows the best of our extrapolation using λ = 0.28. The asymptotic value of the growth exponent from figure 3.5 is $\beta_\infty \approx$ 0.33.

Another quantity that will be discussed is the void defect density. In figure 3.6, the defect density is plotted as a function of the growth time. The results are from 2 systems: L = 900 sites (main plot) and L = 100 sites (inset). The results in figure 3.6 show that the defect density increases rapidly with respect to the growth time in the range from t = 0.2 ML to t = 20 MLs. This is in agreement with the change in the W-t curve (in figure 3.3) from the RD slope to the BD slope. When the time continues longer, the D-t curves saturate at $D(t) \approx 0.54$ for both systems. This means that the film contains approximately 54% of voids inside. This can be seen in figure 3.1 that the film thickness at t = 48 MLs is approximately 100 layers when it should be only 48 layers if the film is grown in the solid-on-solid mode. Previous results [20, 59] show similar behavior. Since the size of the substrate affects the W-t plots, we check to see if it also influences the D-t curves. From systems with L = 100 sites and L = 900 sites in figure 3.6, we do not see any difference. In fact, if we plot the two systems on the same graph, the curves are *exactly* the same. So, it seems that the substrate size does not have any effect on the behavior of the defect density.

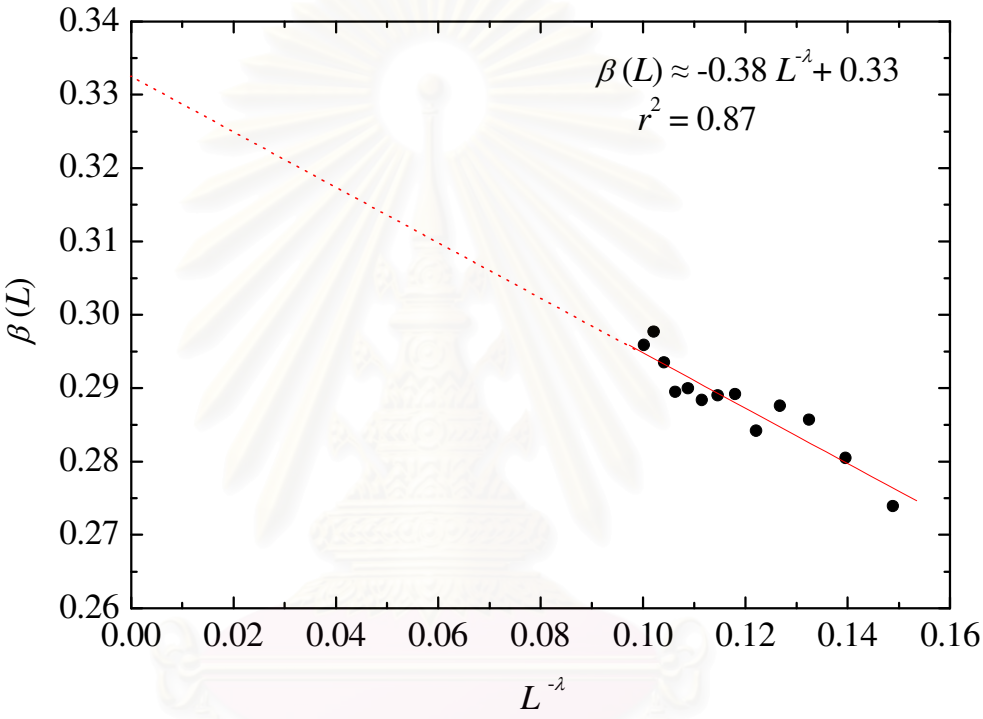

Figure 3.5: The plot of $\beta(L)$ versus $L^{-\lambda}$ of the BD films when $\lambda = 0.28$

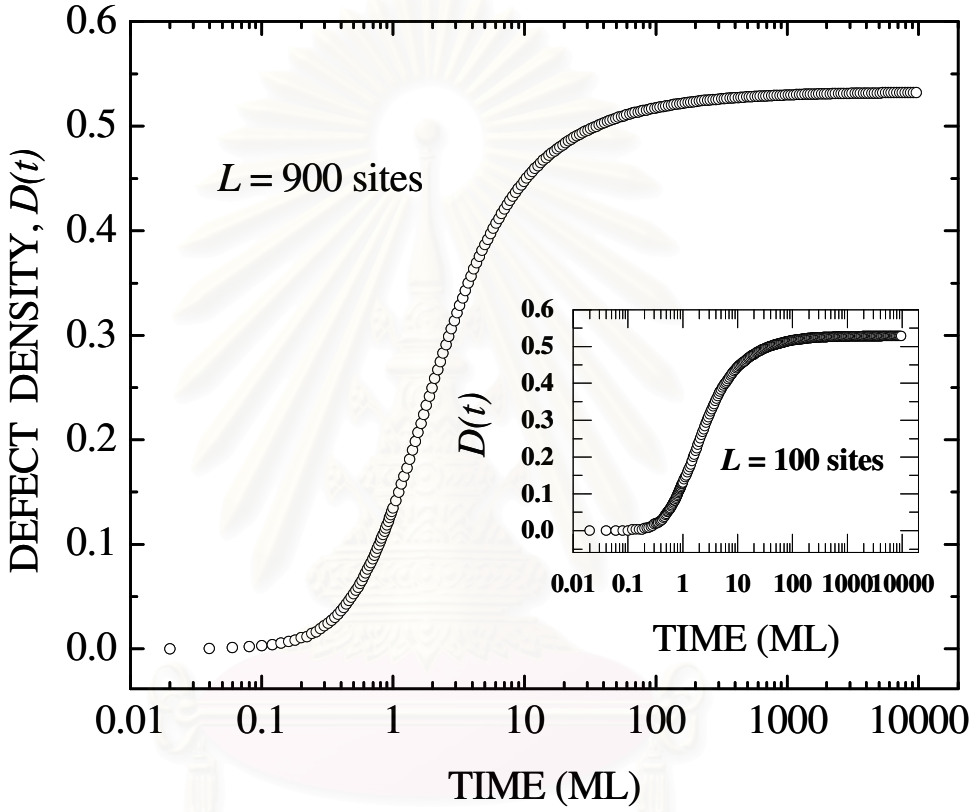

Figure 3.6: The time evolution of the defect densities of the BD films grown in two systems with different substrate sizes

3.1.2 BD model with surface diffusion

Up to this point, we have gained some understanding in the original BD model. Next, we will study the BD model with the surface diffusion process added. As mentioned in Chapter 2, the different interpretation of this surface diffusion process creates two different models which are the conventional model and the realistic model. In this section, their results will be discussed together in order to show the difference between these models. Interested quantities are still similar to those in the previous section: morphology, defect density and interface width.

The simulations from both models show that increasing the substrate temperature leads to the decrease of the void defect density. In figure 3.7, we show our simulated films' morphologies from both models after 50 MLs deposition. It is clear that the "thickness" of films simulated at low temperature is still the same as in the case of original BD model because the surface diffusion process has not been activated when the temperature is too low (T = 600 K for the conventional model and T = 500 K for the realistic model in figure 3.7). But when the temperature is increased, thickness of the films decreases which means the number of voids decreases as well. Here we can see that when the temperature is high enough ($T \geq 700$ K for the conventional model and $T \geq 600$ K for the realistic model) the film thickness is approximately 50 layers which is the number of layers deposited. This behavior is seen in both models. However, it requires higher temperature for the vacancies in the conventional film to be filled because the diffusion of only one particle in the conventional model has much less impact than the diffusion of all surface particles in the realistic model. For example, at T = 600 K, the morphology of the conventional film still has a lot of voids while the morphology of the realistic film shows very few voids inside. So when studying the void defect, both models can provide similar results but at different growth temperatures. This can be confirmed by the overlap plot of defect density versus temperature when the temperature scale is shifted, as shown in figure 3.8. Furthermore, it is obvious from figure 3.7 that increasing the substrate temperature can smooth the film surface. In order to discuss the smoothness/ roughness of the films in detail, the interface widths of both models are plotted versus time in figure 3.9. It can be seen in figure 3.9 that when the temperature is low, the curves are quite similar in both models. From the 600 K system of the conventional model and the 500 K system of the realistic model, we can see that the slope in the

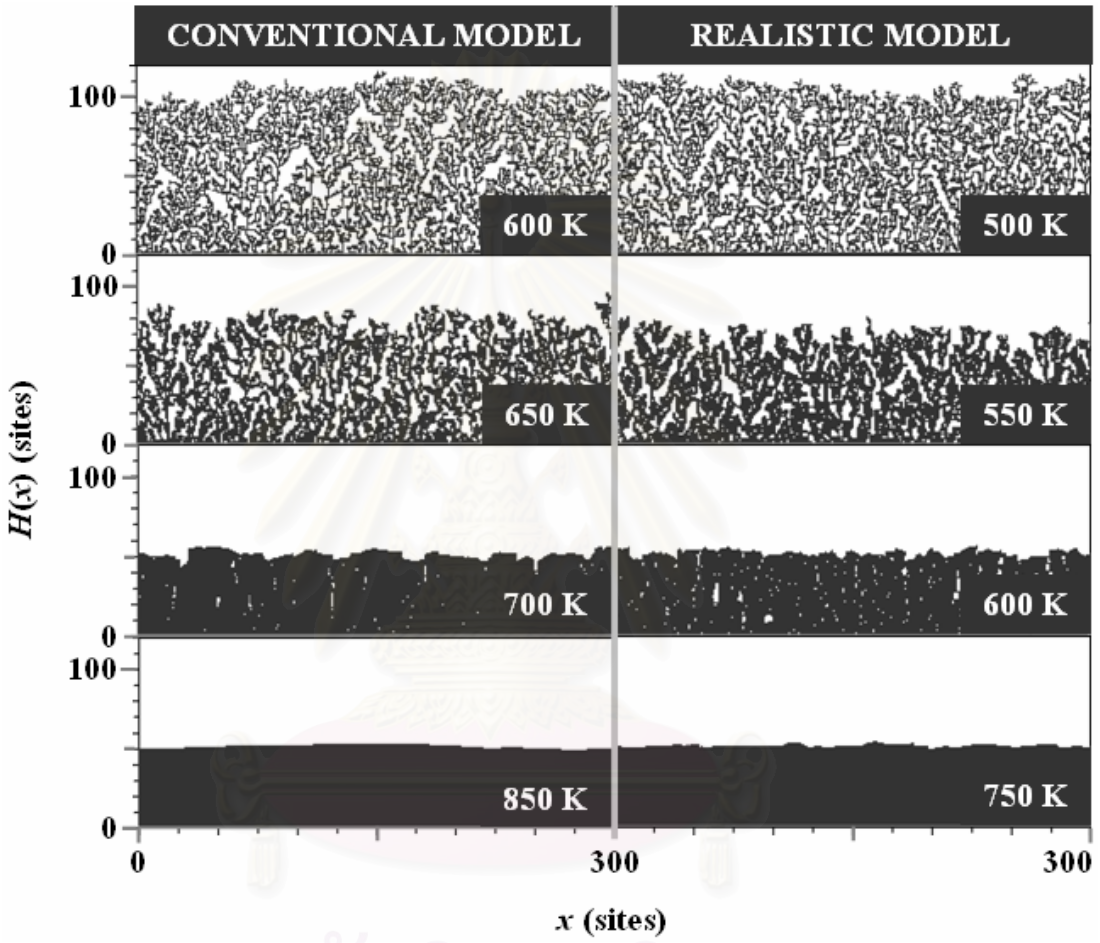

Figure 3.7: Morphologies: A section of 300 lattice sites (from L = 900 sites) from the conventional and the realistic model at various substrate temperatures when t = 50 MLs

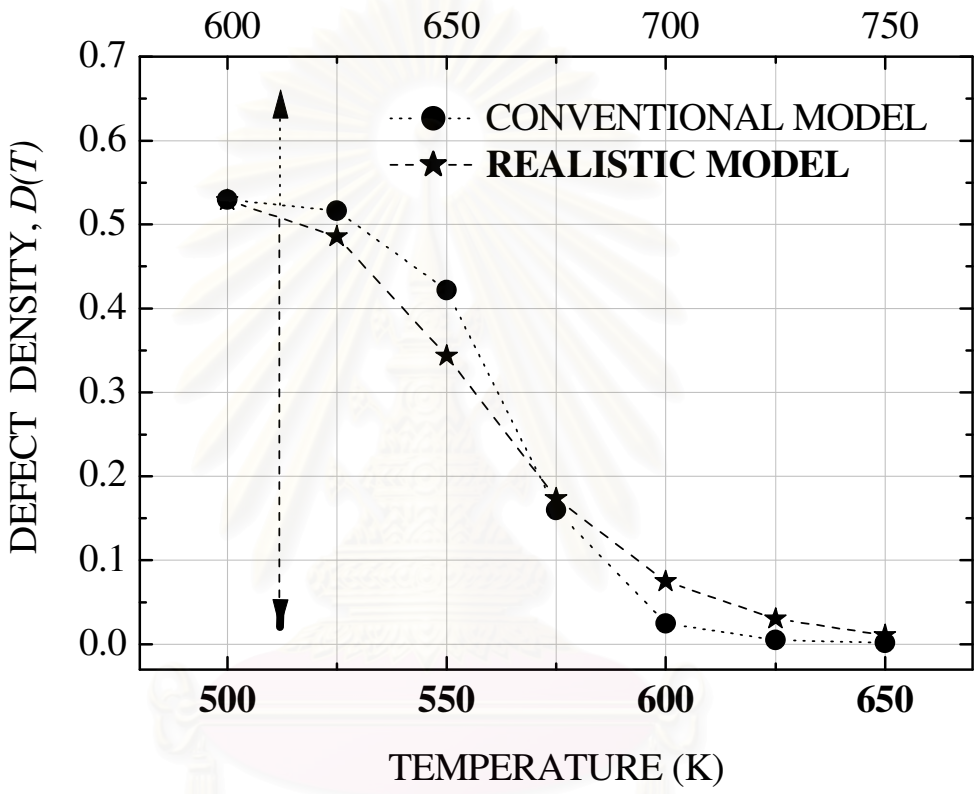

Figure 3.8: The plots of defect density versus substrate temperature of the conventional and the realistic model when L = 900 sites and t = 1000 MLs

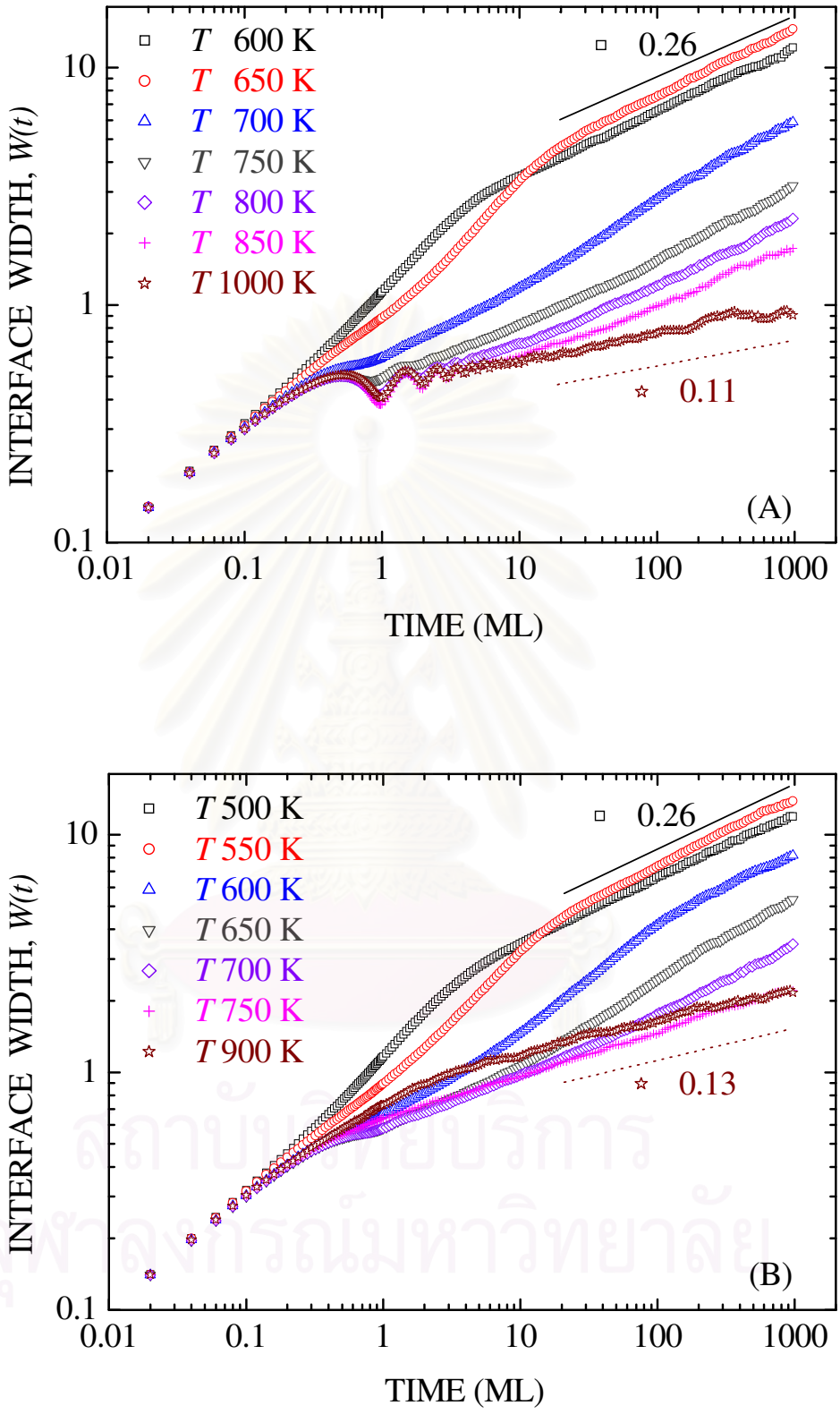

Figure 3.9: The time evolution of the interface widths at various substrate temperatures of the conventional (A) and the realistic (B) films grown on L = 900 sites

second region is still the same as that of the original BD model. This is because, at this level of temperature, the activities on the film are deposition with almost no diffusion. When the temperature is increased, the interface width decreases along with the decreasing of the void defect density. If the temperature is high enough ($T \geq 750$ K in this case), the interface width plots of the conventional model show oscillation in the early time because the diffusing particles have very long surface diffusion length and the film is grown in layer-by-layer mode. This is in accordance with the Reflection High Energy Electron Diffraction (RHEED) oscillation pattern seen in experiments [60-61]. In contrast, the realistic model has not shown any oscillation in the plots even for very high temperature (up to $T = 900$ K). This is likely to be a result of the diffusion of particles with $n = 2$ and 3 that always create new voids and prevent the growth to be layer-by-layer. Hence the interface width for the realistic model maintains the power law relations with the growth time for all values of substrate temperature used in our study.

Another interesting point is shown in figure 3.10 which is the plot of the interface width (at approximately 4 MLs) versus the substrate temperature. It can be seen that when the temperature is increased, the width decreases in both models. However, when the temperature is higher than 700 K, the interface roughness of the realistic films is increased. This is another result arising from the diffusion of particles with $n = 2$ and 3. Similar results were reported in the literatures for the simulation works [43-44] and for the experimental work [62-65]. Since almost all diffusing particles of the conventional model are particles with $n = 1$, this phenomena is not seen in the conventional model. (The curve for the conventional model continues to decrease and then becomes stable in figure 3.10.)

In order to confirm that the oscillation of *W-t* curves at high temperature of the conventional model results from the diffusion of particle with $n = 1$ only, we checked by freezing the diffusion of particles with $n = 2$ and 3 in the realistic model. Figure 3.11 shows the *W-t* plots of the realistic films when the diffusion conditions are adjusted. Solid line (—) shows the plot of the system that allows every kind of particles (particles with $n = 1$, 2 and 3) to diffuse on the film. Open square (□) shows the plot of the system that frozen the diffusion of particles with $n = 3$ while open circular (○) and open triangular (△) plot show the change of systems that do not allows both particles with $n = 2$ and particles with $n = 3$ to diffuse. The results in figure 3.11 show that when the particles with $n = 2$ and $n = 3$ are frozen, the realistic

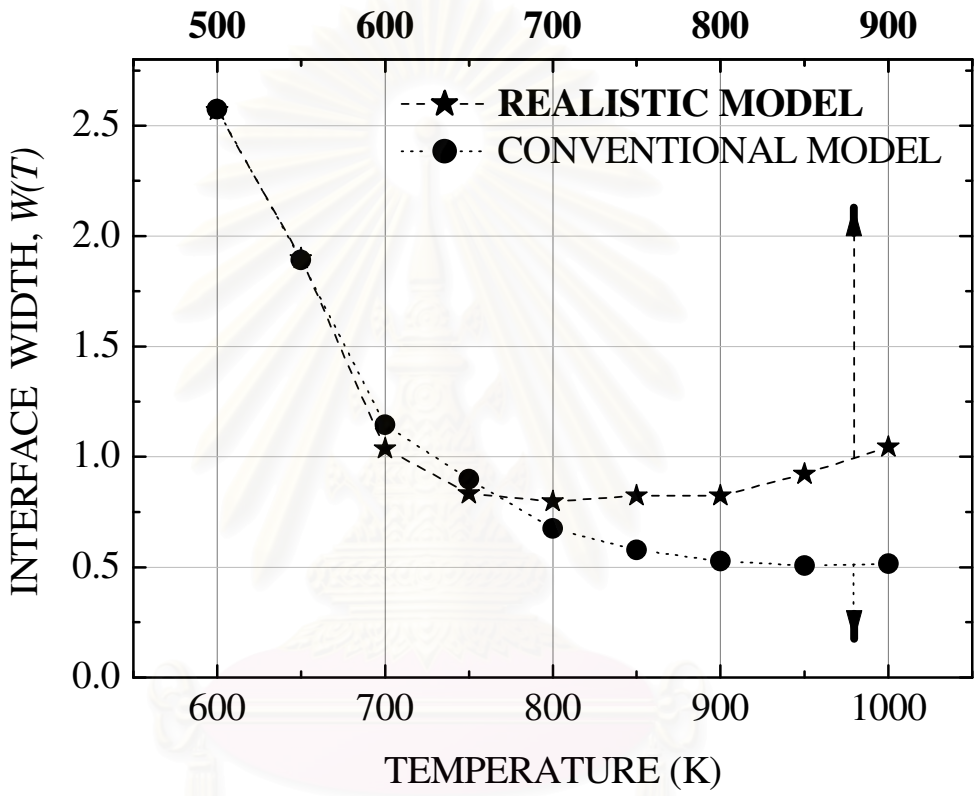

Figure 3.10: The plots of the interface width versus substrate temperature of the conventional and the realistic films grown on $L = 900$ sites at $t \approx 4$ MLs

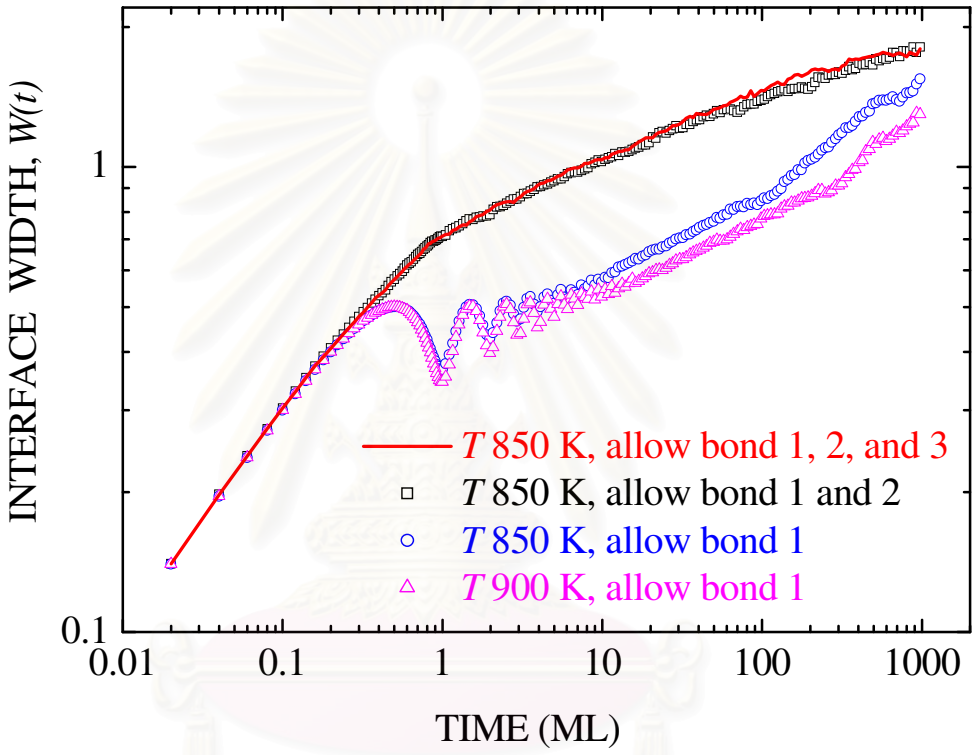

Figure 3.11: The time evolution of the interface width of the realistic films grown on $L = 900$ sites at different growth conditions

curves also oscillate in the same manner as the conventional curves at high temperature in figure 3.9 (A). If the substrate temperature is increased (from T = 850 K to 900 K in this case), the interface roughness plot of the film also decreases similar to the conventional film. These results support our argument in the previous paragraph. Moreover, with similar examination, we also found that the diffusion of particles with n = 3 does not affect the kinetic roughness of the film even in the film that is grown from the realistic model. This can be seen in figure 3.11 that the curve that allows and does not allow the diffusion of particles with n = 3 to diffuse are lined in the same track. This supports the hypothesis of Das Sarma and Temborenea in creating *Das Sarma and Temborenea model* that the diffusion of particle with n = 3 does not impact the growth of the film [66]. Figure 3.12 shows the time evolution of the defect densities in comparison with that of the interface widths. In this figure, we see that the two quantities seem to affect each other in a sense that when the defect density is increasing rapidly ($1 \leq t \leq 10$ MLs for T = 500 K and $1 \leq t \leq 50$ MLs for T = 575 K) the W-t curve undergoes a crossover without a well-defined value for β. When the defect density becomes stable, the W-t plot shows a power law relation again. It also seems that this transition region is stretched out over a longer time period in a system with high substrate temperature.

Another difference in these two models can be found when the temperature of the systems is fixed, but the substrate size L is varied. Figure 3.13, the film morphologies of the conventional and the realistic model grown on different L are compared. In this figure a conventional film with a larger L contains more voids than the films with a smaller L. This is because larger substrate size means higher deposition rate since the deposition rate is fixed that L particles are deposited per unit time in this work. The diffusion rate of only one diffusing particle is, however, independent of the substrate size. Consequently, effects of diffusion compared with effects of deposition are reduced for large L. This is in agreement with previous work [67]. In contrast, from figure 3.13, the realistic model does not show any statistical variation in the films when L is changed since the competition between the deposition and the diffusion rate stays the same.

Finally, we also check to see if our results obey the dynamic scaling hypothesis and the extrapolation relation, in relation (7) and relation (8) mentioned earlier in Chapter 2. In figure 3.14, the W-t plots from simulations at T = 550 K with

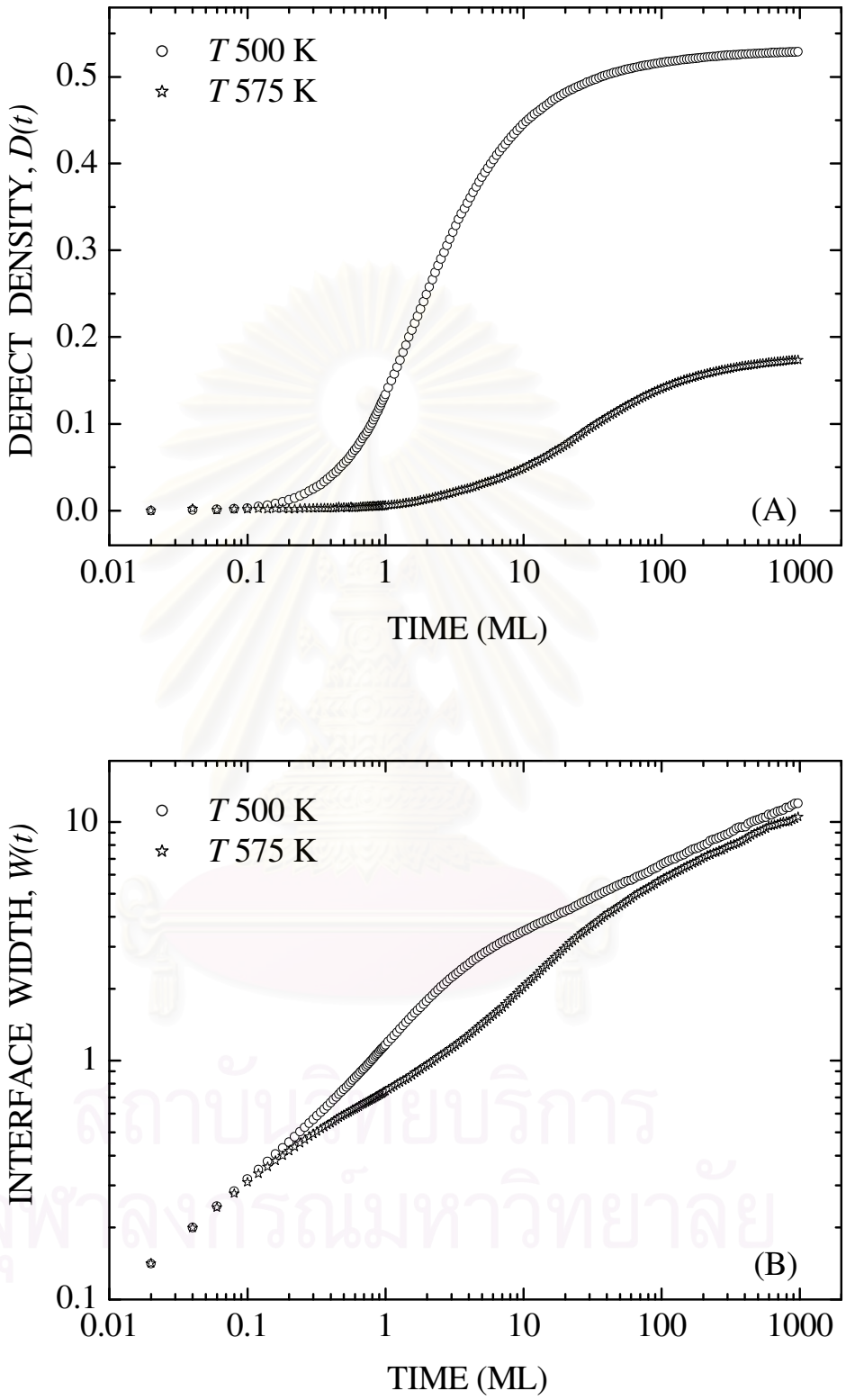

Figure 3.12: The time evolution of the defect densities (A) and the interface widths (B) of the realistic films grown on $L = 900$ sites at two different temperatures

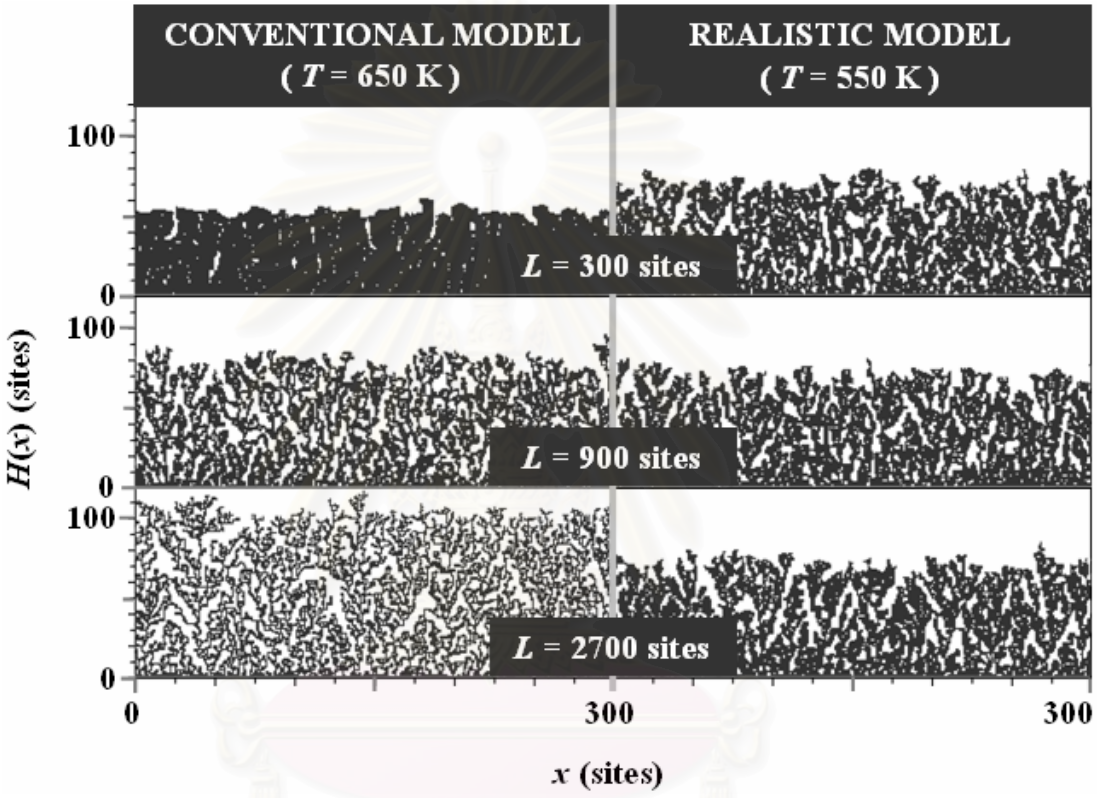

Figure 3.13: Morphologies: A section of 300 lattice sites from the conventional model (at T = 650 K) and the realistic model (at T = 500 K) from various substrate sizes when t = 50 MLs

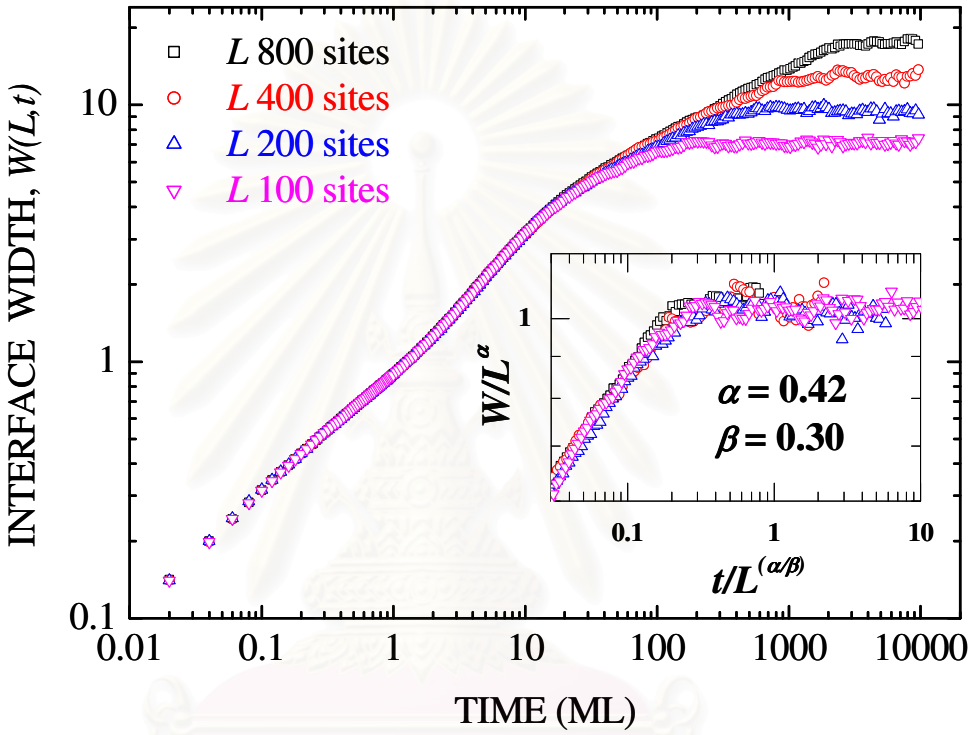

Figure 3.14: The *W-t* plots of the realistic films grown on four different substrate sizes when the temperature is fixed at T = 550 K INSET: The scaling plots of the same systems

various L are shown. The W-t plots of these different system sizes are collapsed onto one line by adjusting the exponents to $\alpha \approx 0.42$ and $\beta \approx 0.30$, as shown in the inset of figure 3.14. This confirms that the BD model with a more realistic approach to the diffusion process still obeys the scaling relation. Moreover, the exponents obtained are still close to the Kardar-Parisi-Zang (KPZ) universality class just as the original BD model. Also, when the temperature is increased to $T = 600$ K, the result still yields $\alpha \approx 0.41$ and $\beta \approx 0.33$ which are not significantly different from the values of α and β at $T = 550$ K. This agrees with the discovery of Yan [59] that the surface diffusion process does not affect the scaling properties of the BD model. Since the slopes of W-t plots in figure 3.14 is also affected from the saturation region as in the case of original BD model, we also used relation (8) to extrapolate the asymptotic value of β (β_∞). Figure 3.15 shows the plot of $\beta(L)$ versus $L^{-\lambda}$ of the films grown from the realistic model. Our result shows that when λ is set to be between 0.39 and 0.44, the data plot is quite linear. Here, β_∞ is approached the theoretical β ($\beta = 1/3$). This result is the same for both the systems that fix $T = 550$ K and $T = 600$ K. However, we note that if the substrate temperature is so high (higher than 700 K in our simulations) that the voids are not created in the film, the value of β decreases down to $\beta \approx 0.11$-0.18 which does not belong to the KPZ universality class. This is obvious because the film contains no void so it is not grown according to the BD model anymore. This result is the same for both the conventional model and the realistic model, as can be seen from figure 3.9 (A) and (B). Also, it is in agreement with the results of Tamborenea and Das Sarma [67].

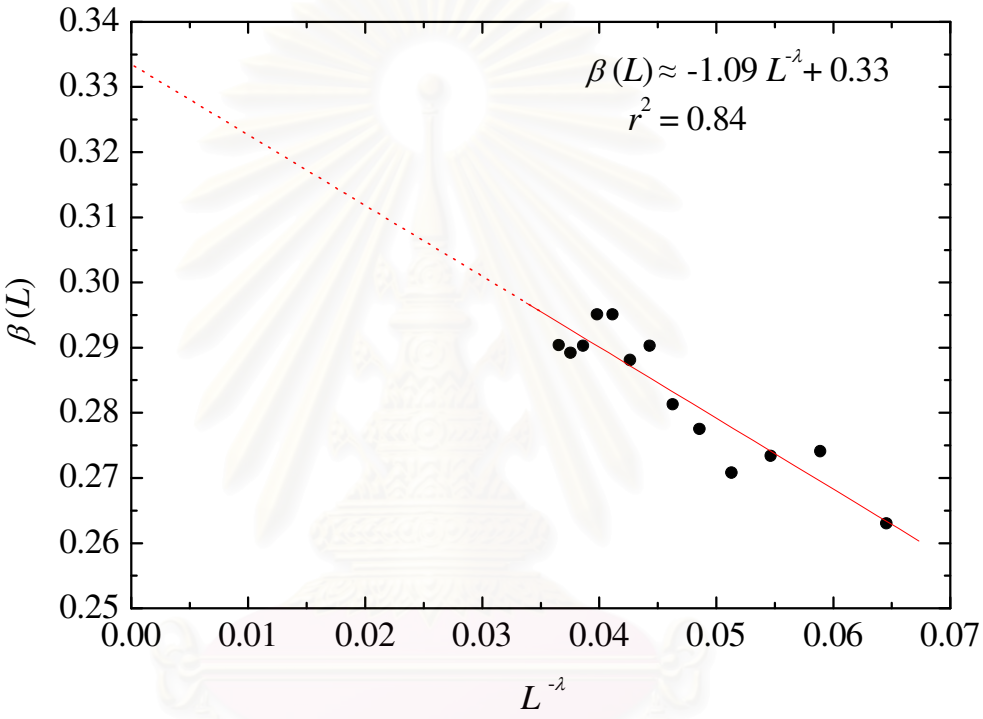

Figure 3.15: The plot of $\beta(L)$ versus $L^{-\lambda}$ of the realistic films when T = 550 K and λ = 0.41

3.2 BD model: Patterned substrates

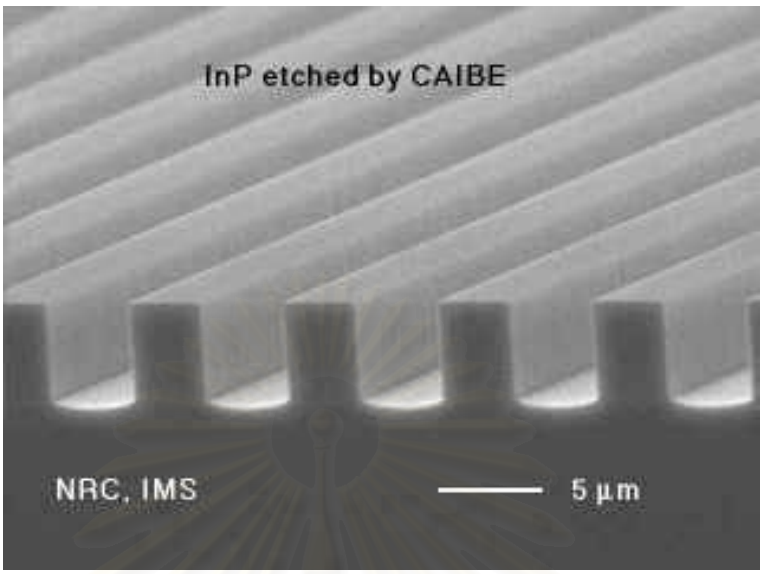

Figure 3.16: A picture of the film etched to produce a periodic pattern. This picture is available from http://www.oxfordplasma.de/process/inp_etch.htm[2008, March 3].

In this section, the ballistic deposition model with surface diffusion is used to simulate films on a patterned substrate. An example of such substrate is shown in figure 3.16. Since this work concentrate on one dimensional film surface, only the cross-section of the substrate is used as our substrates. Here, we can see that if the substrate in figure 3.16 is cut, two types of pattern can be created. The first pattern is a flat pattern which is the cut along the line of the “trail” and the second pattern is a periodic pattern from the cut across the “trial”. The time evolution of the film structure was observed via the film’s morphology and the persistence probability. As discussed in Chapter 2, the modified definition of the persistence probability (equation (10) in Chapter 2) suits better with the films’ morphologies so we chose this formula to use throughout this work. To optimized the unnecessary part of the symbol, $P(t)$ was used instead of $P_n(t)$ because the original definition (equation (9) in Chapter 2) is not used in our work. Since the accepted error (ΔH) is adjustable, we start by choosing $\Delta H = 1$. From the previous section, the different interpretation of the surface diffusion process leads to two different models. However, it is much easier for the discussion in this section if only one model was used. Therefore, the realistic model is selected. For the sake of completeness, the conventional model was also studied. Its results are presented in the last part of this section.

3.2.1 Flat pattern

Flat patterned substrate, in fact, is the substrate without predetermined structure. The details of films that are grown on this type of substrate, e.g. the film morphology, interface width and defect density, have already discussed in the previous section. In this section, the results of persistence probability will be presented. Figure 3.17 shows the time evolution of the persistence probability, $P(t)$, at various substrate temperatures. Here, we can see that, when t increases $P(t)$ decreases in every temperature systems. This is in agreement with the previous section that the height of the film surface (as can be seen from the film morphologies in figure 3.7) deviates from the theoretical value. This is due to the increase of the film roughness. When considering the results of substrate temperature, we can see that increasing T increases the value of $P(t)$. However, if T is higher than 800 K, the $P(t)$ value decreases again. These results can be explained as the following. At low temperature while the diffusion process has not been activated ($T \leq 500$ K), the persistence probability decreases very quickly because at this temperature there are a lot of voids buried inside the film and the height of the film becomes higher than the level it should be. The pattern of the film is damaged rapidly. When the temperature is increased, number of void defect is reduced and the pattern can survive for a longer period of time. At $T = 700$ K, the diffusion rate of the surface particles is appropriate for the vacancies to be filled and for the film surface to be smooth. The pattern of the film can last longest. If the temperature is increased higher than this (e.g. $T = 800$ K), the surface particles will diffuse too fast. This provides chances for a diffusing particle to hop up another surface particle which is already at the upper bound of the accepted range and the persistence probability of that position becomes zero. Although with the high diffusion rate, the particle at the top of the surface can usually come down quickly, by definition, the persistence probability of that position can not be restored. This is why the P-t curves in this temperature region ($T \geq 800$ K) drop faster than the curve at $T = 700$ K, as seen in figure 3.17.

To confirm the explanation above, the morphologies of films grown at $T = 700$ K and $T = 800$ K are investigated. The results are shown in figure 3.18. From this figure, the film surface from $T = 800$ K system is practically the same as the system that $T = 700$ K. This supports our argument that the persistence probability of the 800 K system is small because of the diffusing particles move too much and too fast, and

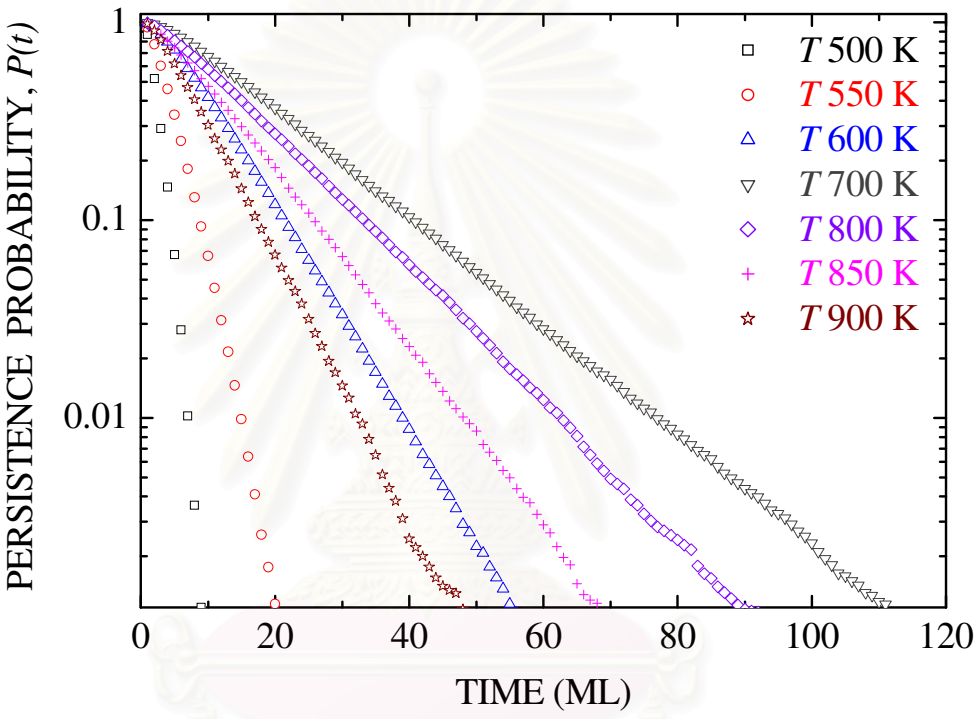

Figure 3.17: The time evolution of the persistence probabilities at various substrate temperatures of the films that were grown on the flat substrate of size L = 900 sites when $\Delta H = 1$

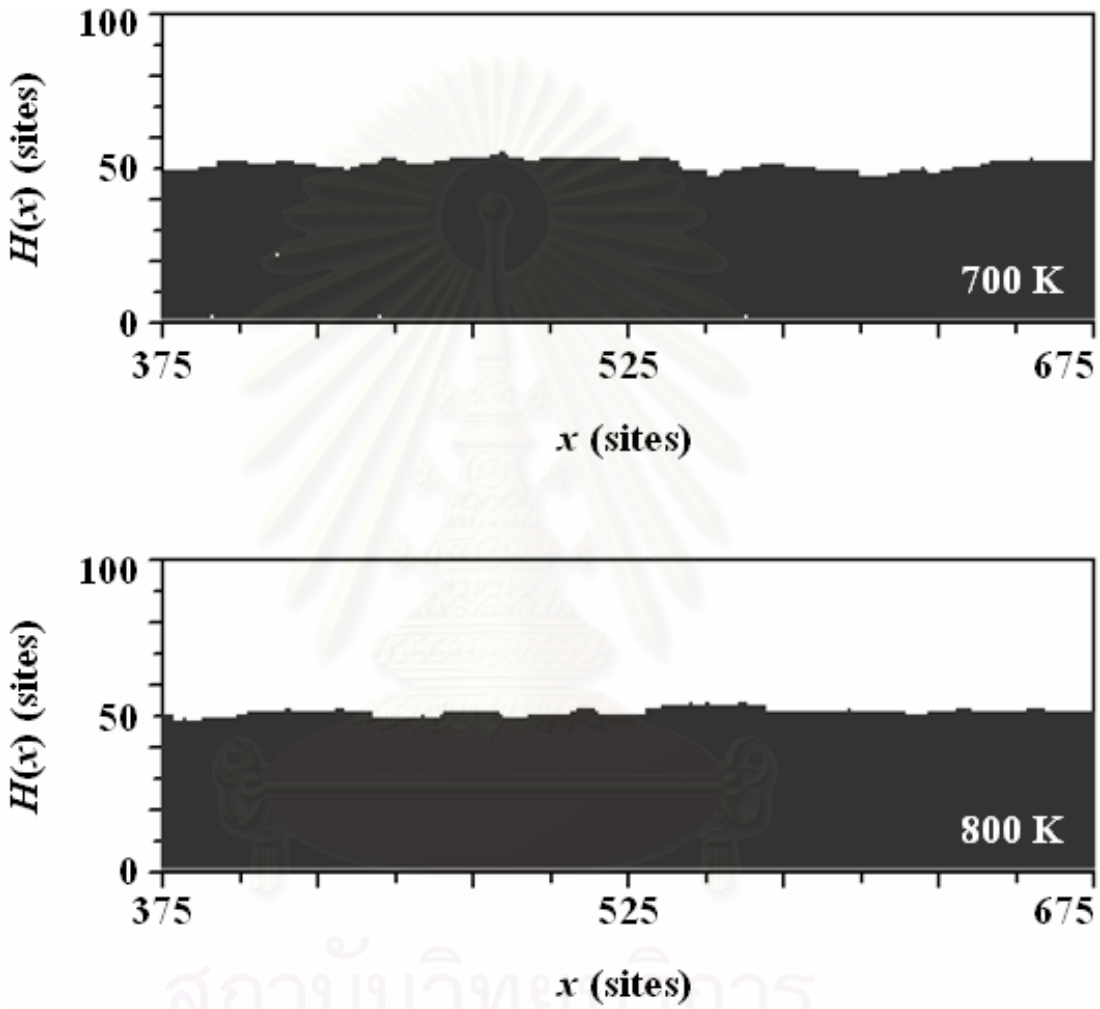

Figure 3.18: Morphologies: A section of 300 lattice sites (from L = 900 sites) of the films grown on the flat substrate at two substrate temperatures when t = 50 MLs

not because the surface of the film is too rough. In order to double check our argument, we increased the accepted error from $\Delta H = 1$ to $\Delta H = 3$. The results are shown in figure 3.19. The *P-t* curves of all temperature systems become larger. Moreover, for system with temperature high enough for the diffusion ($T \geq 700$ K), the value of the persistence probability does not drop too far below the perfect value of $P(t) = 1$. To see the difference between these values of ΔH easier, we plot the persistence probability (at $t = 50$ MLs) as a function of substrate temperature in figure 3.20. In this figure, at low T ($T \leq 550$ K), there is no difference between the curve that $\Delta H = 1$ and the curve that $\Delta H = 3$. This is because the persistence probabilities of both curves decrease down to zero before $t = 50$ MLs, as illustrated in figure 3.17 and figure 3.19. When the temperature is higher than this, the persistence probabilities decrease slower. So, we can see the difference. Here the *P-T* curve that $\Delta H = 3$ is higher than the *P-T* curve that $\Delta H = 1$. The reason is when $\Delta H = 3$, the diffusion of particles at the film surface is confined in the accepted range longer than the case that $\Delta H = 1$. If we take a look at the peak of the curves, we will see that the peak is shifted from $T = 700$ K to $T = 800$ K when we increase ΔH. This can be explained as the following. The roughness of the film can be grouped into two types [44]. The first one is the *kinetic roughness*. It is the roughness that occurs from the random noise in the deposition process. At low temperature, when the growth time increases, this roughness is also increased. This is why it is named the kinetic roughness. The second roughness is the *thermal roughness*. It is a result of the diffusion process of surface particles. For example, if a surface particle of the perfectly smooth film hops up onto its nearest-neighbor particle, the surface height at its pervious position will decrease while that at its new position will increase. This results in the roughening of the film surface. Since this process is driven by the temperature of the substrate, this parameter is used to name this roughness. When the temperature of the substrate is increased until the surface diffusion process dominates the deposition process, the roughness of the film will be the thermal roughness. Although the thermal roughness destroys the film pattern faster than the kinetic roughness when ΔH is small ($\Delta H = 1$ in this case) because of the dynamic of the film surface, the amplitude of thermal roughness is smaller than that of the kinetic roughness. Thus, when ΔH is increased from $\Delta H = 1$ to $\Delta H = 3$, the *P-t* curve at $T = 800$ K is decreased slower than that at $T = 700$ K. Since $\Delta H = 3$ gives the *P-t* curve that is more consistent with the film morphologies, we decided to use $\Delta H = 3$ for the rest of this work unless otherwise noted.

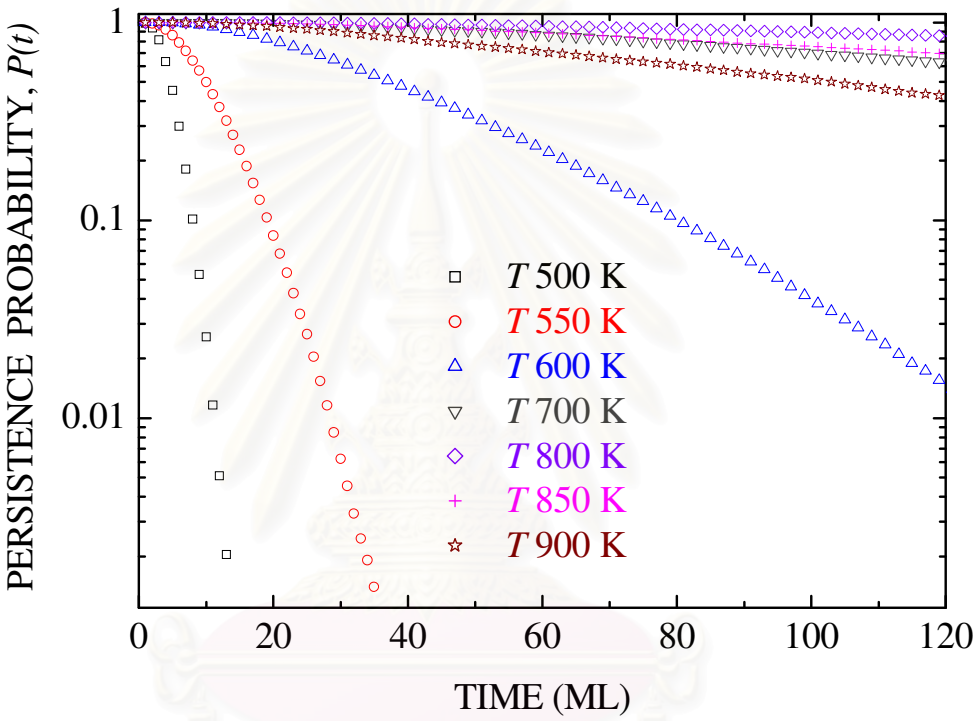

Figure 3.19: The time evolution of the persistence probabilities at various substrate temperatures of the films that were grown on the flat substrate of size L = 900 sites when $\Delta H = 3$

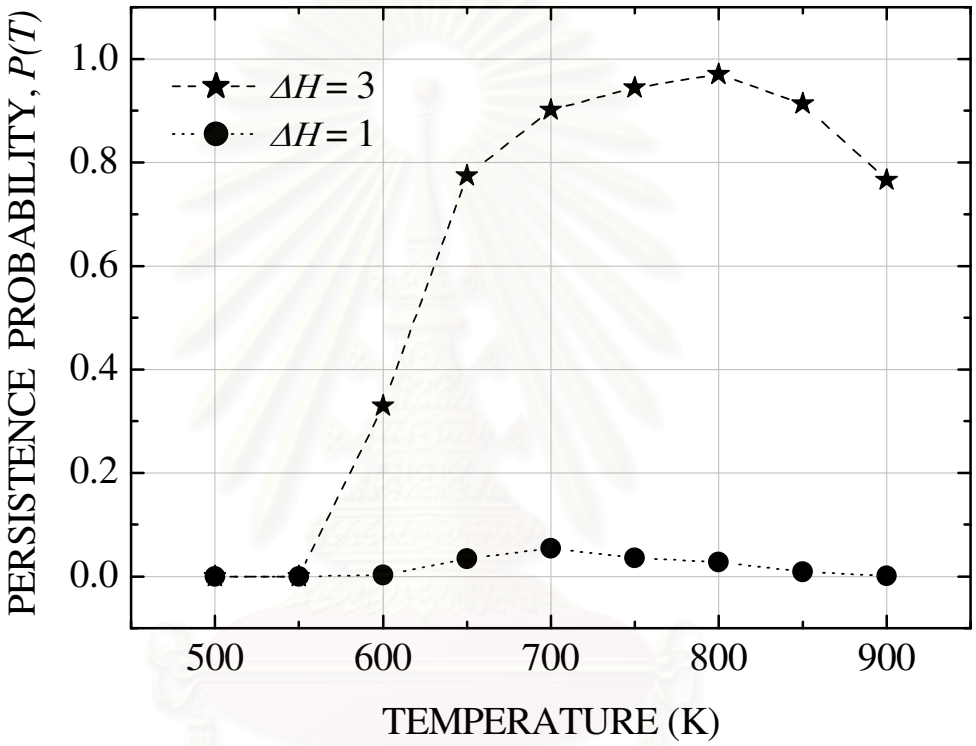

Figure 3.20: The plots of the persistence probability versus substrate temperature of the films grown on the flat substrate of size $L = 900$ sites at $t \approx 50$ MLs

3.2.2 Periodic pattern

For the growth on periodic patterned substrates, all growth conditions are set to be the same as those of the flat patterned substrates except the structure of the substrate which is a series of blocks as shown in figure 3.21. Here, we set both the width of the blocks (W_B) and the width of the grooves (W_G) at 150 sites and the height of these blocks (H_B) at 90 sites. The substrate size (L) still is 900 sites. The film morphology and the persistence probability are quantities of interest in this part.

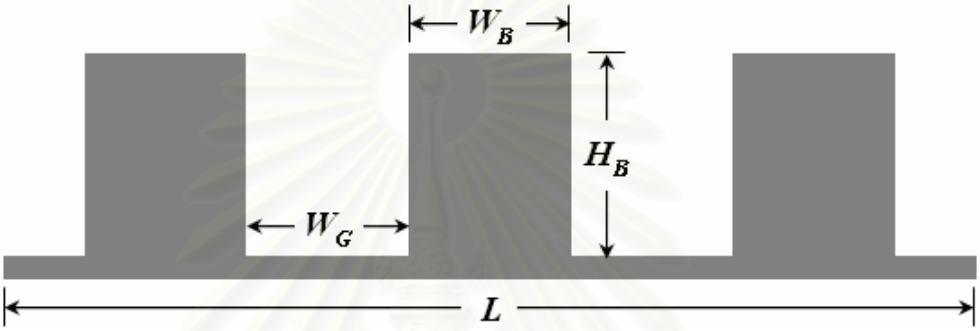

Figure 3.21: A schematic diagram showing a periodic patterned substrate

3.2.2.1 Morphologies

The morphologies of films grown on periodic patterned substrates are studied here. Figure 3.22 shows the time evolution of the film grown at T = 500 K when the growth time is paused at t = 90 MLs—different shades represent different time interval which is 30 MLs. From this figure we found that, for the periodic patterned substrate at very low substrate temperature ($T \leq 500$ K), the original BD rules which allow overhanging of deposited particles can affect the growing film immediately after the growth process starts. This is in contrast with the flat substrate growth that the effect can be seen after approximately 0.2 ML. The reason is if the first particle is deposited at a position that its side touches the wall of a block on the substrate, it will stop there and create a large space under it. Newly arrived particles can not go under this particle and the space can not be filled anymore because the temperature is too low for particles to diffuse. When the growth time continues longer, more particles are deposited. The overhanging parts from the blocks expand wider like tree branches until they cover the grooves. The growing films in the grooves are completely covered; therefore, they stop growing. As a result, the thickness of films in these grooves is non-uniform. In figure 3.22, we can see that the thickest part of the film in

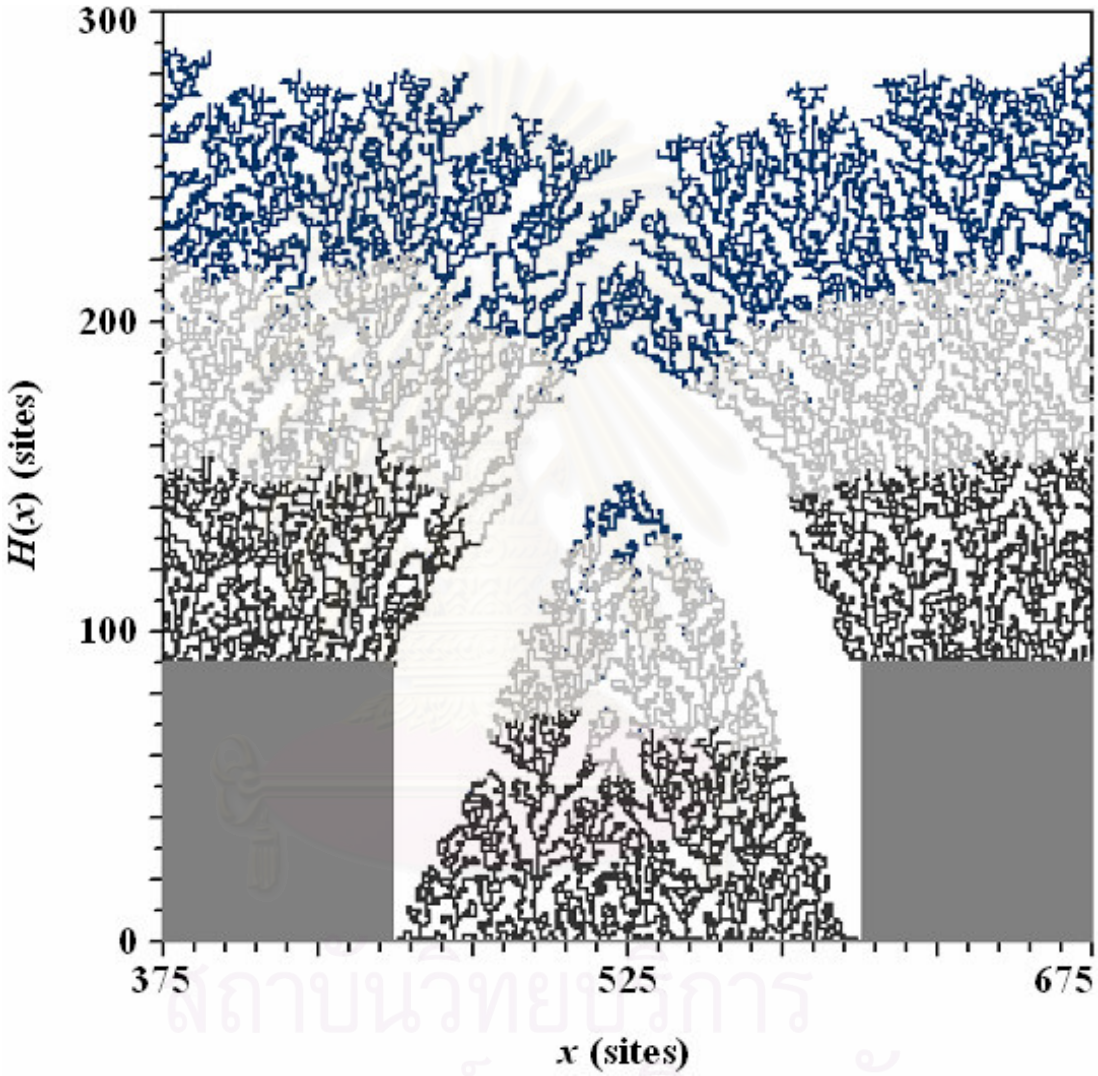

Figure 3.22: Morphology: A section of 300 lattice sites (from L = 900 sites) of the films grown on the periodic patterned substrate at T = 500 K when t = 90 MLs. Different shades represent different time intervals: the shading changes after every 30 MLs.

the groove is located at the middle part of the groove because this is the last part that is covered. After the growing films on the blocks covered the grooves, the films will be grown as if they are on a flat substrate. Our result agrees well with an experiment by Karabacak and Lu [68]. In their experiment, Ruthenium (Ru) film is deposited on a trench structure with the aspect ratio 2:1 (400 nm height and 200 nm width). The scanning electron microscope (SEM) image of this film is shown in figure 3.23. It can be seen from figure 3.23 that the experimentally grown film is very similar to the morphology of our simulated film in figure 3.22. The films on the blocks expand like the branch of tree, the film thickness in the grooves is non-uniform, and there are large voids at the groove's corners. The only difference between these films is that there is a "side wall" growth in the experimentally grown film in figure 3.23 while there is no such thing in the simulated film in figure 3.22. This is because the deposition beam in the experiment makes an angle θ with the substrate, but the model used here assumes the beam of depositing particle is normal to the substrate.

In figure 3.24, morphologies of films grown to t = 50 MLs on the periodic substrate at various substrate temperatures are shown. As we have discussed earlier, when the temperature is increased, the surface particles can diffuse to fill the voids in the film. With this diffusion process, the volume of the film is decreased. The overhanging parts of the films on the blocks are smaller and it takes longer time for the grooves to be covered. Therefore, the part of the film in these grooves can be grown longer and the thickness of the film in the grooves is more uniform, as can be seen in the figure. When T approaches 700 K, almost all the void defect is reduced. The lateral growth rate decreases. The film's morphology looks very similar to the morphology of the substrate. If the temperature is higher than this (T = 850 K in the figure), the average distance where the diffusing particle can diffuse to (*the surface diffusion length*) is increased. The particles located on the top of the blocks can move down to the grooves and tend to stay here for a long time. The reason is when these particles (particles with n = 1) reach a site located at a corner between the wall of a block and the plane of a groove, their bonding number increases to n = 2 and their diffusion rate decreases. So, they take longer time for the next diffusion to occur and it provides great opportunities for other diffusing particles to land on top and buries them. When the time progresses longer, the number of particles that diffuse down to the grooves becomes larger and the film thickness at the edges of the grooves becomes larger as well. This is in contrast with the film thickness on the blocks,

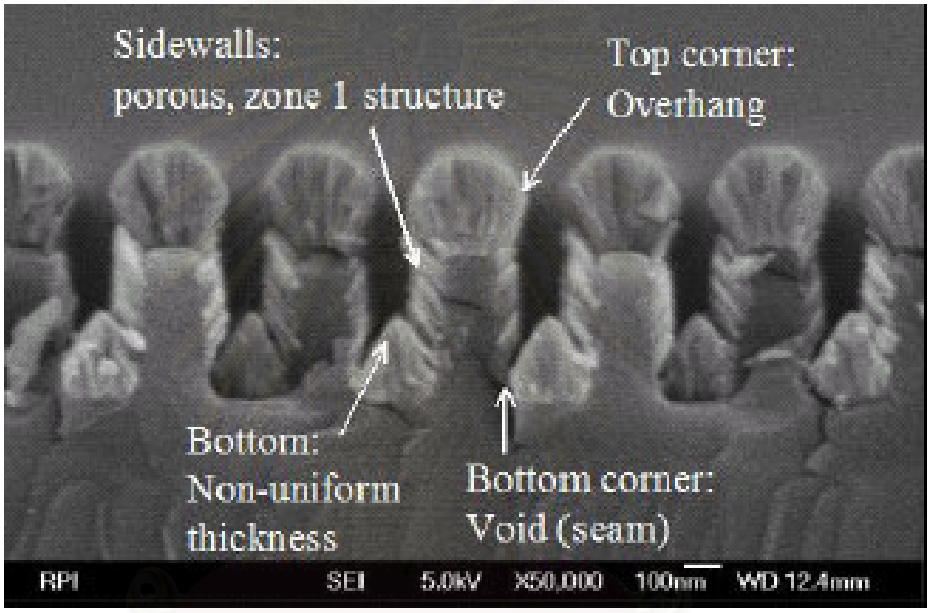

Figure 3.23: The copied photo of Karabacak and Lu [68] showing the cross-section of SEM image of the Ru film deposited on 2:1 aspect ratio (400 nm height and 200 nm width) trench structures at the highest substrate temperature $T \approx 358$ K

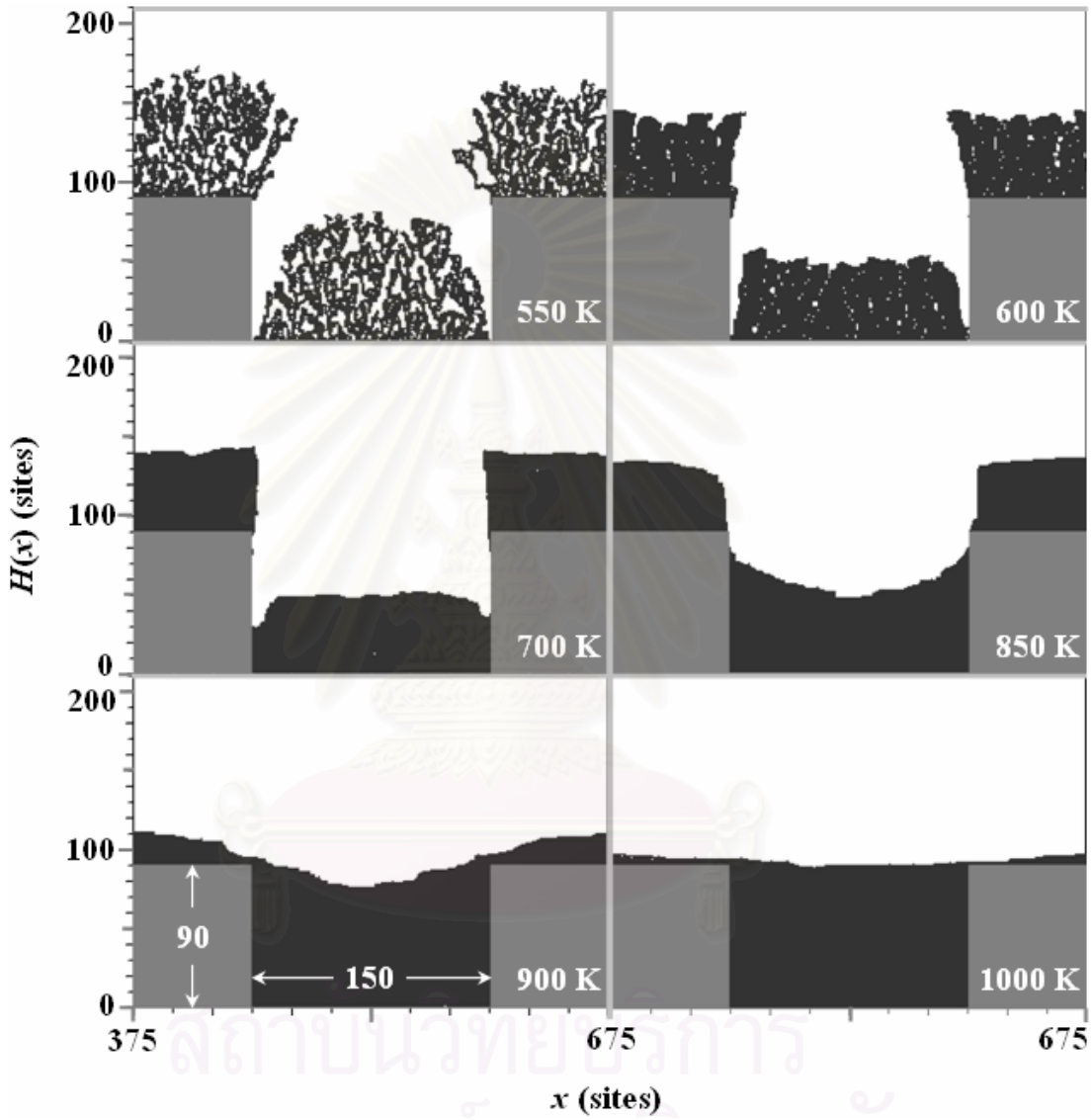

Figure 3.24: Morphologies: A section of 300 lattice sites (from L = 900 sites) of the films grown on the periodic patterned substrate at various substrate temperatures when t = 50 MLs

where the particles near the edge of the blocks hop down. So the heights of the film near the edge of the blocks are less than the expected value. This is why the film's pattern is damaged rapidly. These effects are more obvious when T = 900 K. If the temperature is still increased (e.g. at T = 1000 K in figure 3.24), the diffusion length of the diffusing particles is very long (longer than the width of the blocks) and all particles deposited on the block can diffuse down to the grooves at the instant that they reached the film surface. When the growth time evolves to approximately half the height of the substrate (t = 50 MLs for the cases in figure 3.24), the grooves of the film will be filled completely. The film surface becomes flat. After that the film will be grown as if it is on the flat substrate.

In conclusion, our results show that at low temperature the pattern is destroyed quickly from the void defect. On the other hand, at high temperature, the diffusion length of diffusing particles is too long and that destroy the pattern just as quick. From the morphologies, it is clear that there is only a small range of temperature that is suitable for growth on periodic patterned substrates. To be more quantitative, the persistence probability is discussed in the next part.

3.2.2.2 Persistence probabilities

In figure 3.25 the persistence probabilities as a function of the growth time are shown. When considering these persistence probabilities, we found that at $T \leq 700$ K the change of the curves (in figure 3.25) is the same as that of the flat films (in figure 3.19) although. However, the films' morphologies are different. The reason is, at this temperature, the influence of void defect is much stronger than the influence of the substrate's structure. So, the film surface becomes thick faster than the accepted level before the effect of overhang is shown. If the temperature is increased further, the void defect decreases. The surface diffusion length is larger. The film surface is leveled off according to the migration of the particles from the blocks to the grooves. The film's pattern is damaged; therefore, the persistence probability decreases. Since the effect of initial structure is more powerful than that of thermal roughening. The persistence probabilities of the periodic films decrease faster than that of the flat films. This can be seen clearly from the curve of T = 850 K in figure 3.25 in comparison with the curve of the same temperature in figure 3.19. The turning point

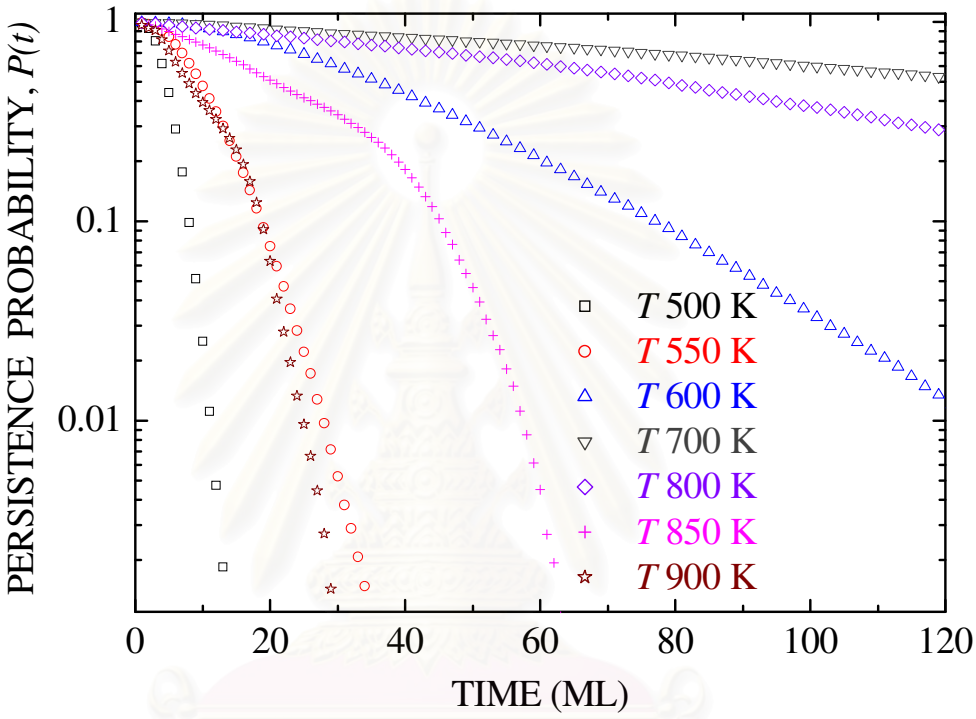

Figure 3.25: The time evolution of the persistence probabilities at various substrate temperatures of the films grown on the periodic patterned substrate of size L = 900 sites

at t approximately 40 MLs of the curve in figure 3.25 shows the time that the pattern of films on the blocks is totally destroyed. Here, almost all patterns of the film are demolished; the persistence probability decreases rapidly. In figure 3.25, we can also see that increasing the substrate temperature moves the turning point up to an earlier time. This is a result of the long surface diffusion length of the diffusing particles as predicted by Piankoranee [41, 57].

In order to see the effect of the initial structure more clearly, the persistence probabilities of both the flat and the periodic films are plotted as a function of the substrate temperature. This is shown in figure 3.26. From this figure, the difference can be observed starting from T = 700 K. The difference becomes more pronounce at higher temperature ($T \geq 750$ K). For the flat film, when T increases, the P-T curve changes slightly; in contrast, the same curve of the periodic film decreases rapidly. If we take a look at the peak of the graph of the periodic film, we will see that the peak is at $T \approx 700$ K. Also, the peak of the graph of the flat film is at $T \approx 800$ K. These confirm that, for the growth on any patterns of the substrate, there is only a very short range of temperature that the film can maintain its original pattern for a long time.

To better understand in the effect of the original structure, we also studied the growth on different pattern size. Here, we separate the variation into three cases. In the first case, we set the width of the blocks (W_B) equals to the width of the grooves (W_G) which is equal to a constant, and then vary the height of the blocks (H_B). The second case is fixing H_B, but varies W_B. Here W_B is still equal to W_G. Finally, in the third case, all variables are set the same as the second case except that $W_B \neq W_G$. Since the effect of the original structure can be seen more clearly when $T \geq 700$ K and the curve at T = 850 K suits the best with the change in this temperature region in our study, we choose T = 850 K as the fixed temperature throughout our study in this part. The substrate size is still kept at the same size as the previous part (L = 900 sites).

For the first case, W_B is fixed at 150 sizes but H_B is varied from 90 sites to 180 sites. Figure 3.27 shows the time evolution of the persistence probabilities of the film grown on the substrate with H_B = 90 sites and another film grown on the substrate with H_B = 150 sites. From this figure, we found that the reduction of the persistence probabilities in both cases is nearly the same in the early growth time (the first 20 MLs). The reason for this is that the migrations of particles from the blocks that have the same width in both cases are equal. So, the damaged parts are quite the same.

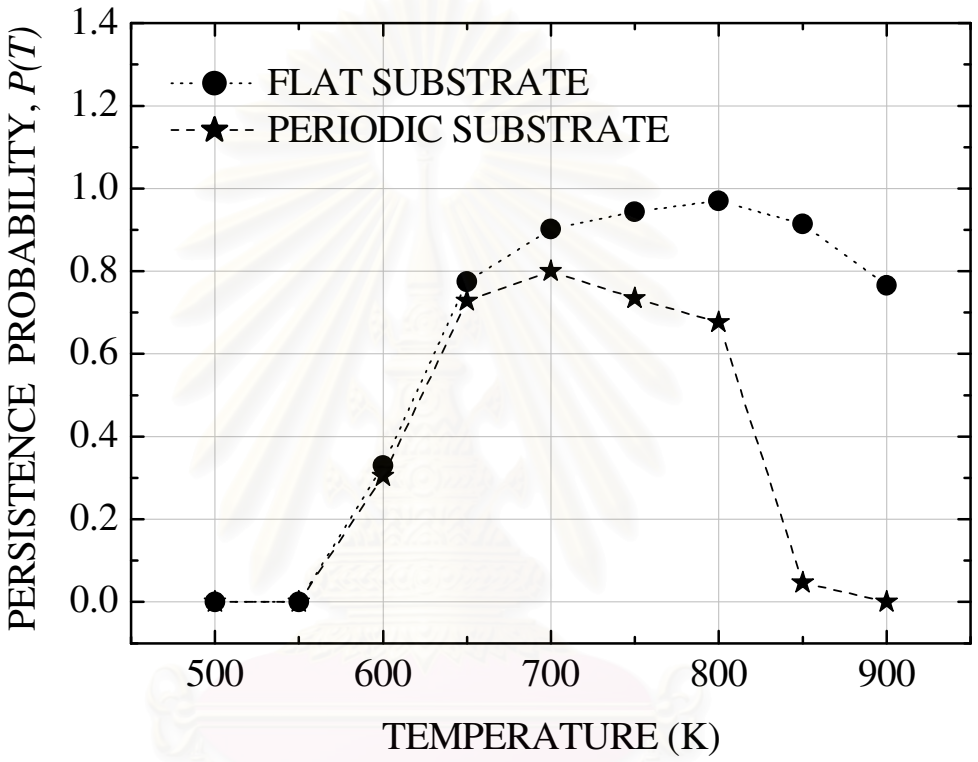

Figure 3.26: The plots of the persistence probability versus substrate temperature of the films grown on the flat and the periodic patterned substrate when L = 900 sites and t = 50 MLs

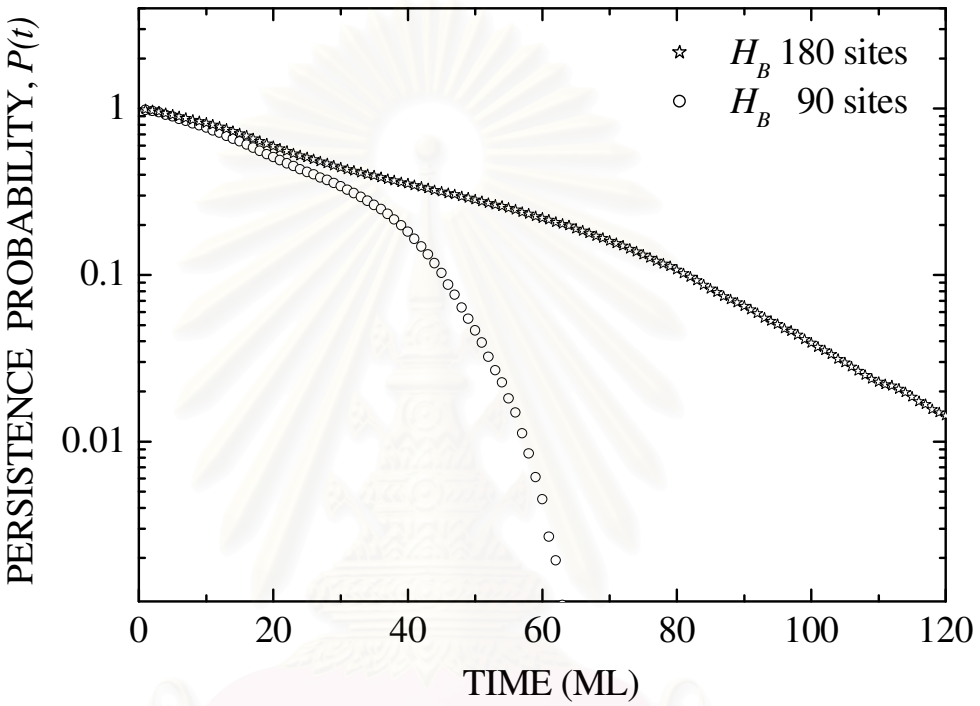

Figure 3.27: The time evolution of the persistence probabilities at T = 850 K of the films grown on two periodic patterned substrates of size L = 900 sites when the widths of the patterns are fixed at $W_B = W_G$ = 150 sites

However, if the time continues longer, it is shown that the pattern with higher H_B can maintain its original structure longer. This is because the particles on the blocks take longer time to diffuse down to the grooves. The pattern of films on the grooves is destroyed slower.

In the second case, H_B is fixed at 90 sites but W_B (which is equal to W_G) is increased from 75 sites to 150 sites. Figure 3.28 shows the plot of persistence probability versus time of the films grown on the periodic patterned substrates which have two different W_B. The first substrate has W_B = 75 sites while another substrate has W_B = 150 sites. From this figure, the persistence probability of the film grown on the substrate with larger W_B can stay at a large value for a long time, and longer than the substrate with smaller W_B. This is because the particles on the blocks have larger area to move on before they fall into the grooves. Therefore, the original pattern of this kind of film can be kept better than the pattern of the film grown on the substrate with smaller W_B.

In the third case, the height of the blocks is fixed at H_B = 90 sites and the widths of the pattern, W_B and W_G, are varied. Figure 3.29 shows our results from three sets of pattern's widths: W_B = 225 sites / W_G = 75 sites, W_B = 15 sites / W_G = 150 sites and W_B = 75 sites / W_G = 225 sites. From this figure, we can see that the pattern with either W_B or W_G equals to 225 sites can maintain the original structure longer than the pattern with $W_B = W_G$ = 150 sites. This is because the impact from the migration of particles at the edge of the blocks destroys the film's pattern at the middle parts of the larger flat parts slower when either W_B or W_G is larger. As a result, the persistence probabilities in these cases decrease slower. On the other hand, if the consideration takes place only when $W_B \neq W_G$, we found that the change of the curves can be separated into two regions. In the first region, the curve of the pattern which has $W_B > W_G$ can maintain its value longer. The reason for this is that when the diffusing particles on the blocks diffuse down to the narrow grooves, they will be confined in small areas. The larger flat parts of the pattern which are outside the grooves are affected slowly. Thus, the film surface can remain in the accepted range longer. In the second region, the curve with $W_G > W_B$ decreases slower because the edge effect impacts the middle part of the grooves slower than the middle part of the blocks. The particles at the edge of the grooves, which has always $n > 1$, diffuse to the middle part of the grooves slower than the migration of particles, which has always $n = 1$, from the blocks to the grooves.

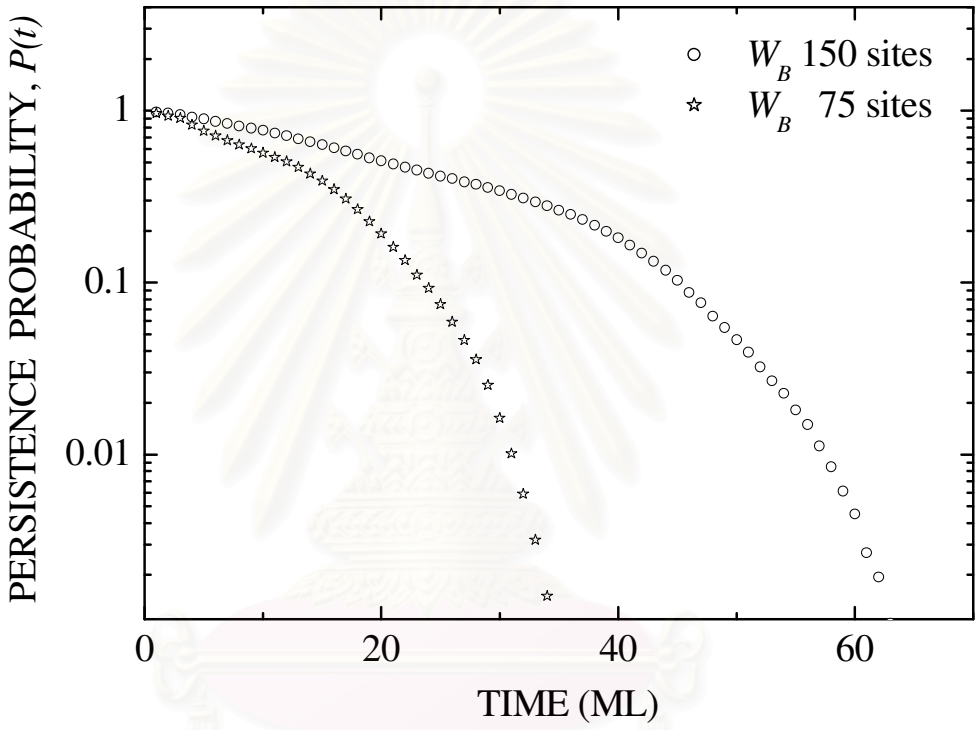

Figure 3.28: The time evolution of the persistence probabilities at T = 850 K of the films grown on two periodic patterned substrates of size L = 900 sites when H_B is fixed, but W_B which is equal to W_G is varied

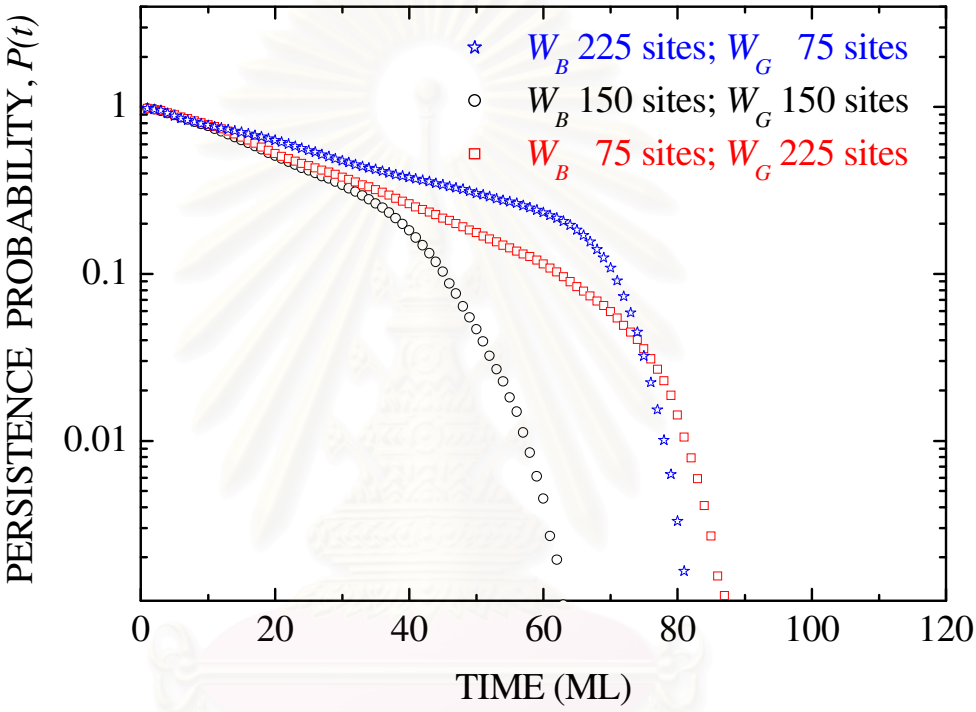

Figure 3.29: The time evolution of the persistence probabilities at T = 850 K of the films grown on three periodic patterned substrates of size L = 900 sites when the widths of the patterns are varied

3.2.3 Conventional model vs. Realistic model

In the growth on patterned substrates, the different interpretations of the surface diffusion process are also considered. Figure 3.30 presents the plots of $P(t)$ versus time of the conventional films grown on the flat substrate when the accepted error is fixed at $\Delta H = 1$, but the substrate temperature is varied. From this figure, the persistence probabilities of the conventional films show similar change as that of the realistic films except at very high temperature ($T > 800$ K for the conventional films and $T > 700$ K for the realistic films). In this temperature region, instead of decrease, the persistence probabilities of the conventional films increase with the temperature of the substrate even when $\Delta H = 1$. This shows that the higher the temperature, the smoother the conventional film surface. This is in agreement with the results discussed earlier when the interface width of the films is studied. If ΔH is increased to $\Delta H = 3$, the *P-t* curves are decreased slower, as in the case of the realistic film.

Figure 3.31 shows the plots of persistence probability as a function of substrate temperature of the conventional and the realistic films grown on the flat substrate when $\Delta H = 3$. From this figure, the difference between the models can be seen more clearly especially at high temperature region. In this region, the realistic curve decreases when the temperature is increased higher than 800 K while that of the conventional model at equivalent temperature still remains stable. This is due to the different surface diffusion rules as discussed in the *W-t* plots in figure 3.10.

When the conventional films are grown on the pattern that has $W_B = W_G = 150$ sites and $H_B = 90$ sites, we found that the films' morphologies vary with the substrate temperature like those of the realistic films. However, the temperature required for the change is different. At low temperature, when the film still contains voids, the conventional films require 100 K higher than the realistic films in order to get the similar morphologies. This result is the same as the result of the films grown on the flat substrate in figure 3.7. On the other hand, when $T > 800$ K (for the conventional film), the temperature requirement is changed. Here, we found that the change from $T = 1000$ K to $T = 1100$ K of the conventional film is similar to the change from $T = 850$ K to $T = 900$ K of the realistic film in figure 3.24. Here, the conventional film requires 100 K for the change while the realistic film requires only 50 K. The reason for this difference is that the overall diffusion of the conventional particles is smaller than that of the realistic particles. Therefore, the conventional particles are distributed

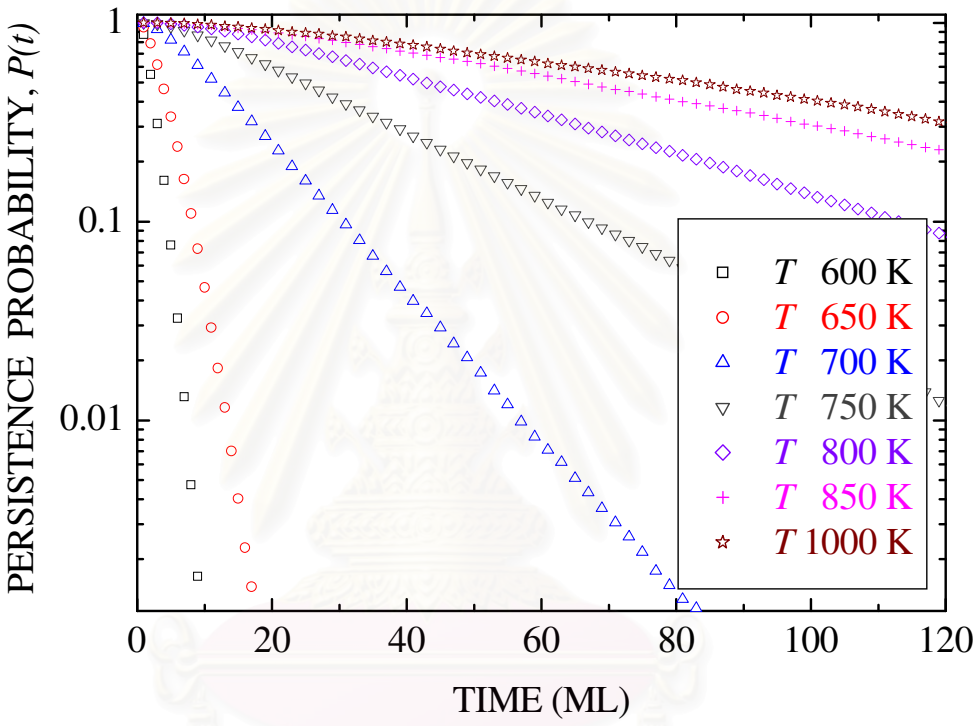

Figure 3.30: The time evolution of the persistence probabilities at various substrate temperatures of the conventional films grown on the flat substrate of size L = 900 sites when ΔH = 1

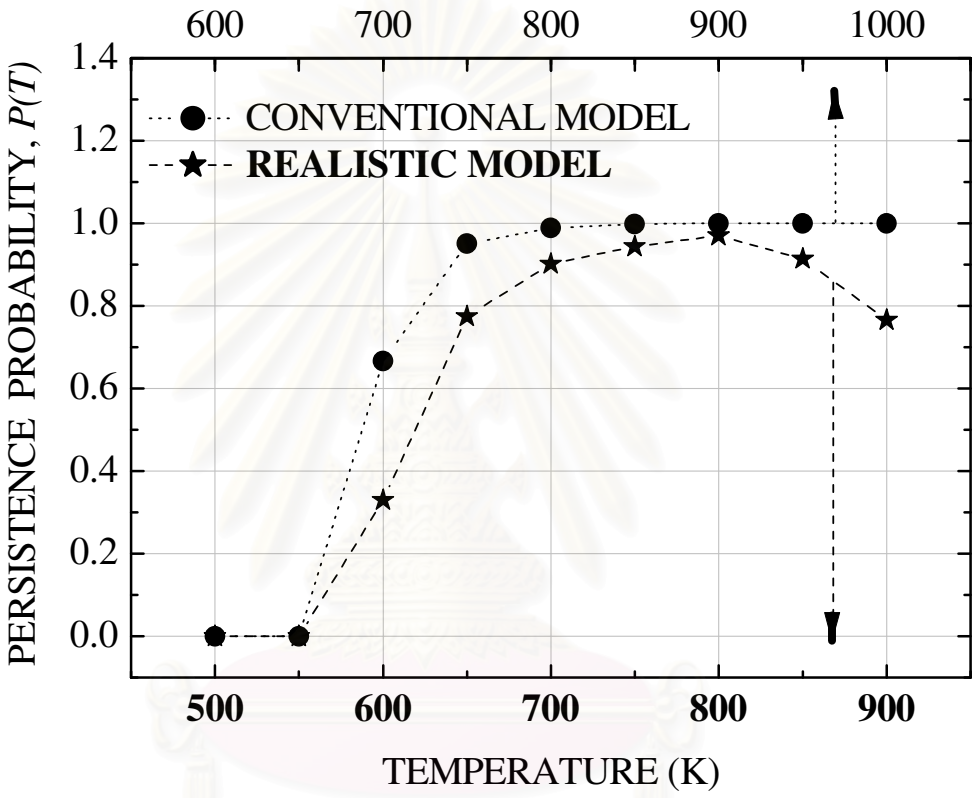

Figure 3.31: The plots of the persistence probability versus substrate temperature of the conventional and the realistic films grown on the flat substrate of sizes L = 900 sites when ΔH = 3 and t = 50 MLs

over the entire film surface slower than the realistic particles. This is why the conventional film's morphology requires higher temperature for this change. On the contrary, for the change from T = 1100 K to T = 1150 K of the conventional film which is relevant to the change from T = 900 K to T = 1000 K of the realistic film (in figure 3.24), the conventional film requires lower temperature than the realistic film. This is because, in this temperature region, the overall diffusion of the conventional particles can compete with that of the realistic particles. Also, the realistic model allows the diffusion of particles with n = 2 and n = 3 which tend to increase the roughness of the film as shown in figure 3.10. Therefore, the conventional film's morphology is changed faster.

Figure 3.32 shows the *P-t* curves of the conventional films grown on the periodic patterned substrate when ΔH = 3. When considering the results in this figure in comparison with the same results of the realistic film in figure 3.25, we found that if the film morphologies are similar, the *P-t* curves of both films are nearly the same. However, this does not include the case of conventional film at T = 1000 K and the case of realistic film at T = 850 K. Although these film morphologies are similar at t = 50 MLs, their *P-t* curves are different. Here we can see that the *P-T* curve of the conventional model has two breaking points while the *P-T* curve of the realistic model has only one. This can be explained from figure 3.33 as the following. The first breaking point of the conventional curve is a result of the destruction of the film's pattern on the blocks of the substrate. At this temperature, the diffusion length of the surface particles is longer than the width of the blocks. When a particle is deposited on the blocks, there will be two chances for the particle to diffuse. The first chance is completing the film's layer if that particle touches a kink site on the block of the substrate. The second chance is diffusing down to the groove of the substrate. Since, in this temperature region, the conventional film is grown in the layer-by-layer growth mode, the film surface is smooth at all time. Most particles that deposited on the blocks are diffused down to the grooves suddenly they reached the film surface. Thus, the pattern of the films on the blocks is grown very slower than the accepted range. The persistence probabilities of the films on these blocks decrease rapidly. This is why we can see the first breaking-point in the conventional curve. However, for the particles that diffuse down to the grooves, they tend to stay at the grooves' borders for a long time. The film thickness at the middle parts of the grooves is destroyed slowly,

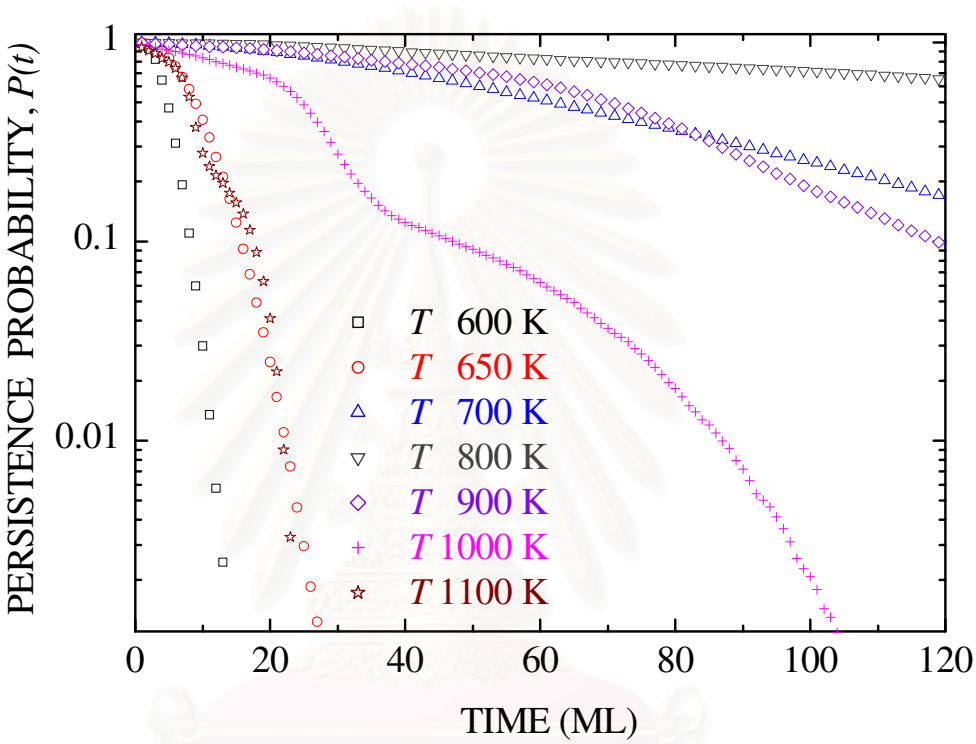

Figure 3.32: The time evolution of the persistence probabilities at various substrate temperatures of the conventional films grown on the periodic patterned substrate of size $L = 900$ sites when $\Delta H = 3$

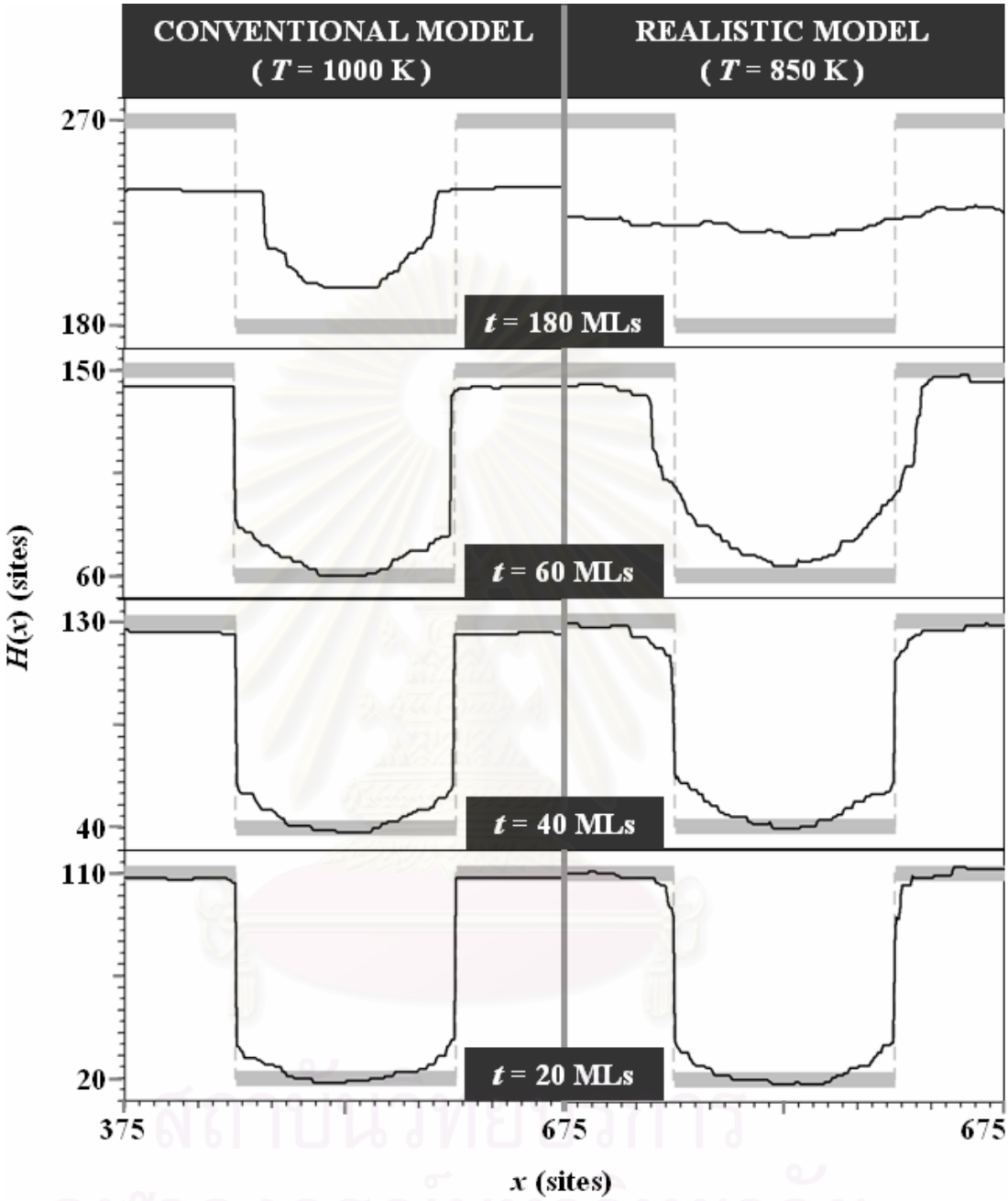

Figure 3.33: Surface Morphologies: A section of 300 lattice sites (from L = 900 sites) of the conventional and the realistic film grown on the periodic patterned substrate at different growth time

slower than the destruction of the film thickness at the middle parts of the blocks. So, the persistence probabilities of the films in these grooves decrease slower. This causes the second breaking point in the conventional film's curve. On the other hand, for the realistic model, all surface particles can diffuse at a time. The diffusion of surface particles is distributed over the entire film surface. The pattern of the films both on the blocks and in the grooves of the substrate are destroyed in the same rate. This is why we can see only one breaking point in the realistic curve at T = 850 K in figure 3.25. Moreover, figure 3.33 also shows that, at t = 60 MLs, the conventional film's morphology on the blocks of the substrate can still keep the original structure of the substrate although the persistence probability is totally reduced. In contrast, this can not be seen in the realistic film. This is due to the different diffusion rules of the models which make the conventional film grows in layer-by-layer mode in this temperature region while the realistic film can not. At t =180 MLs, the conventional film's morphology shows the expansion of the block size according to the heap of the migrated particles. Here, the width of the blocks is increased, but the film surface at these parts still smooth. This is in accordance with the results of Piankoranee [57] because of the consistence of the diffusion rules, the diffusion of only one particle at a time. On the contrary, we can not see this effect in the growth of the realistic film. If the time processes longer, both the conventional film and the realistic film are grown as they are on the flat patterned substrate. Since the change of the realistic film is faster than the change of the conventional film, this effect can be seen faster as shown in the realistic film's morphology in figure 3.33 (at t = 180 MLs).

Chapter 4
Conclusions

The main purpose of this work is to study the growth of porous thin film on substrates with predetermined structure. A ballistic deposition model with thermally activated surface diffusion process was used in this study. During producing the model, an ambiguity of the added process raised us two different interpretations which result in two different models. The first model is the conventional model and the second model is the realistic model. The comparative study between these two models emphasizes that the surface diffusion process is a temperature dependence process as it is predicted from the theory. Therefore, different conditions of this process can be seen only when substrate temperature is high enough for surface particles to diffuse. Here, we found that at moderate temperature the realistic model requires lower temperature for vacancies to be filled. Also, the deposition rate of this model does not depend on the size of the substrate which is in contrast with the conventional model. At high temperature, the difference is clearer. The film surface of the conventional model is grown in layer-by-layer fashion and it is very smooth for all high temperature simulations. On the contrary, we do not find layer-by-layer growth in the realistic model. As the temperature is increased, the film becomes smooth, but when the temperature is increased further, the film becomes rough again.

When using the realistic model to study the growth on patterned substrates, we found that the persistence probabilities of the films grown on both flat and periodic substrates decrease with growth time. When the time is fixed, the substrate temperature plays an important role in controlling the film's pattern. Here, we found that, at low temperature, the major effect destroying the film's pattern during growth is the void defect. This result is the same for the growth on both the flat and the periodic substrates. On the other hand, if the temperature is high enough for surface particles to diffuse, the main effect becomes the surface diffusion process. When the temperature is increased, the persistence probability of the flat film increases and tends to keep stable at higher temperature. In contrast, the persistence probability of the periodic film decreases when the temperature is higher than the suitable level at

which the diffusing particles have just completely filled the void and smoothed the film surface. When the size of the periodic pattern is varied, we found that the pattern with larger flat parts can maintain the original pattern longer. These results are similar for both the growth from the conventional and the realistic model.

In order to get a more realistic prediction, we plan to expand our study to 2+1 dimensional growth mode, and also plan to use our models to study some extra factors related to the growth, e.g. the Erlich-Shwobel barrier. Since the results from our two different models match well with the experimental results at high temperature, we also plan to combine the significant features of both the conventional model and the realistic model into one new model.

References

[1] M.J. Vold, *J. Colloid Sci.* 14 (1959): 168.

[2] D.N. Sutherland, *J. Colloid Interface Sci.* 22 (1966): 300.

[3] M.E. Kainourgiakis, E.S. Kikkinides, T.A. Steriotis, A.K. Stubos, K.P. Tzevelekos and N.K. Kanellopoulos, *J. Colloid Interface Sci.* 231 (2000): 158.

[4] R. Karmakar, T. Dutta, N. Lebovka and S. Tarafdar, *Physica A* 348 (2005): 236.

[5] S. Sadhukhan, T. Dutta and S. Tarafdar, *J. Stat. Mech.* (2007): 6006.

[6] P. Lavalle, J.-F. Stoltz, B. Senger, J.-C. Voegel and P. Schaaf, *Proc. Nat. Acad. Sci. U.S.A.* 93 (1996): 15136.

[7] J.E. Yehoda and R. Messier, *Appl. Surf. Sci.* 22 (1985): 590.

[8] P. Meakin, P. Ramanlal, L.M. Sander and R.C. Ball, *Phys. Rev. A* 34 (1986): 5091.

[9] R.N. Tait, T. Smy and M.J. Brett, *Thin Solid Films* 187 (1990): 375.

[10] S.W Levine, J. R. Engstrom and P. Clancy, *Surf. Sci.* 401 (1998): 112.

[11] B.J. Bartholomeusz and T.K. Hatwar, *Thin Solid Films* 181 (1989): 115.

[12] L. Vázquez, R.C. Salvarezza, P. Herrasti, P. Ocón, J.M. Vara and A.J. Arvia, Appl. *Surf. Sci.* 70 (1993): 413.

[13] P. Carl, M. Schmittbuhl, P. Schaaf, J.-F. Stoltz, J.-C. Voegel, B. Senger, *Physica A* 298 (2001): 198.

[14] Z. Dohnálek, G.A. Kimmel, P. Ayotte, R.S. Smith and B.D. Kay, *J. Chem. Phys.* 118 (2003): 364.

[15] R. Buzio, A. Chierichetti, G. Bianchi and U. Valbusa, *Surf. Coat. Technol.* 200 (2006): 6430.

[16] R. Dasgupta, S. Roy, S. Tarafdar, *Physica A* 275 (2000): 22.

[17] K. Trojana, M. Ausloosb, *Physica A* 326 (2003): 492.

[18] Y. Enomoto and M. Taguchi, *Appl. Surf. Sci.* 224 (2005): 213.

[19] T. Panczyk, T.P. Warzocha, W. Rudzinski, *Appl. Surf. Sci.* 254 (2008): 2285.

[20] S. Das Sarma, C.J. Lanczycki, S.V. Ghaisas and J.M. Kim, *Phys. Rev. B* 49 (1994): 10693.

[21] C.J. Lanczycki and S. Das Sarma, *Phys. Rev. B* 51 (1995): 4579.

[22] R.N. Esfahani, G.J. Maclay, G.W. Zajac, *Thin Solid Films* 219 (1992): 257.

[23] R.W. J. Chia, C.C. Wang and J.J.K. Lee, *J. Magn. Magn. Mater.* 209 (2000): 45.

[24] G.W. Bryant, *J. Lumin.* 70 (1996): 108.

[25] K. Shiralagi, R. Zhang and R. Tsui, *J. Cryst. Growth* 201 (1999): 1209.

[26] S. Watanabe, E. Pelucchi, B. Dwir, M. Baier, K. Leifer and E. Kapon, *Physica E* 21 (2004): 193.

[27] S. Ohkouchi, Y. Nakamura, N. Ikeda, Y. Sugimoto and K. Asakawa, *J. Cryst. Growth* 301 (2007): 744.

[28] M. Nishioka, S. Tsukamoto, Y. Nagamune, T. Tanaka and Y. Arakawa, *J. Cryst. Growth* 124 (1992): 502.

[29] Y. Oda, T. Fukui, *J. Cryst. Growth* 195 (1998): 6.

[30] C. Jiang, T. Muranaka and H. Hasegawa, *Microelectron. Eng.* 63 (2002): 293.

[31] A. Ueta, K. Akahane, S. Gozu, N. Yamamoto, N. Ohtani and M. Tsuchiya, *J. Cryst. Growth* 301 (2007): 846.

[32] Y. Hanein, Y.V. Pan, B.D. Ratner, D.D. Denton and K.F. Böhringer, *Sens. Actuators, B* 81 (2001): 49.

[33] Y. Fu, H. Du and J. Miao, *J. Mater. Process. Technol.* 132 (2003): 73.

[34] D.-C. Lim, H.-G. Jee, J.W. Kim, J.-S. Moon, S.-B. Lee, S.S. Choi, J.-H. Boo, *Thin Solid Films* 459 (2004): 7.

[35] Z. Yang, R. Wang, D. Wang, B. Zhang, K.M. Lau and K.J. Chen, *Sens. Actuators, A* 130 (2006): 371.

[36] J.R. Lawrence, P. Andrew, W.L. Barnes, M. Buck, G.A. Turnbull and I.D.W. Samuel, *Appl. Phys. Lett.* 81 (2002): 1955.

[37] D. Pisignano, L. Persano, P. Visconti, R. Cingolani, G. Gigli, G. Barbarella and L. Favaretto, *Appl. Phys. Lett.* 83 (2003): 2545.

[38] J.R. Lawrence, G.A. Turnbull, I.D.W. Samuel, *Appl. Phys. Lett.* 82 (2003): 4023.

[39] M. Gaal, C. Gadermaier, H. Plank, E. Moderegger, A. Pogantsch, G. Leising and E.J.W. List, *Adv. Mater.* 15 (2003): 1165.

[40] H. Kallabis and D. Wolf, *Phys. Rev. Lett.* 79 (1997): 4854.

[41] S. Piankoranee and P. Chatraphorn, *J. Sci. Res. Chula. Univ.* 3 (2005): 131.

[42] G.H. Gilmer and P. Bennema, *J. Appl. Phys.* 43 (1972): 1347.

[43] R.-F. Xiao, J.I.D. Alexander, and F. Rosenberger, *Phys. Rev. A* 43, (1991): 2977.

[44] R.-F. Xiao and N.-B. Ming, *Phys. Rev. E* 49 (1994): 4720.

[45] R.W. Smith and D.J. Srolovitz, *J. Appl. Phys.* 79 (1996): 1448.

[46] M. Castro, R. Cuerno, A. Sánchez and F. Domínguez-Adame, *Phys. Rev. E* 62 (2000): 161.

[47] Y. Kaneko, Y. Hiwatan, K. Ohara and T. Murakami, *Surf. Coat. Technol.* 169 (2003): 215.

[48] A.-L. Barabási and H.E. Stanley, *Fractal Concepts in Surface Growth*, Cambridge University Press, Cambridge, 1995.

[49] R.M. D'Souza, Int. *J. Mod Phys C* 8 (1997): 941.

[50] R.M. D'Souza, Y. Bar-Yam and M. Kardar, *Phys. Rev. E* 57 (1998): 5044.

[51] W.H. Press, S.A. Teukolsky, W.T. Vetterling, B.P. Flannery, *Numerical Recipes in C, The Art of Scientific Computing*, 2nd Ed. (Acrobat Ed.), *Numerical Recipes Books On-Line*, Cambridge University Press, 1992. Available from: http://www.nrbook.com/a/bookcpdf/c7-1.pdf[2008, March 3]

[52] M. Karda, G. Parisi and Y. Zhang, *Phys. Rev. Lett.* 56 (1986): 889.

[53] F. Family and T. Vicsek, *J. Phys. A* 18 (1985): L75.

[54] F.D.A. Aarão Reis, *Phys. Rev. E* 63 (2001): 56116.

[55] R. Miranda, M. Ramos and A. Cadilhe, *Comput. Mater. Sci.* 27 (2003): 224.

[56] H. Kallabis and D. Wolf, *Phys. Rev. Lett.* 79 (1997): 4854.

[57] S. Piankoranee, *Persistence in Thin Film Growth on Patterned Substrates*, Master Thesis, Faculty of Science, Chulalongkorn University, 2005.

[58] F. Family, *Physica A* 168 (1990): 561.

[59] H. Yan, *Phys. Rev. Lett.* 68, (1992): 3048.

[60] I.K. Marmorkos and S. Das Sarma, *Phys. Rev. B* 45 (1992): 11262.

[61] W. Braun, *Applied RHEED Reflection High-Energy Electron Diffraction During Crystal Growth*, Springer, Germany, 1999.

[62] S.G. Yoon, H.K. Kim, M.J. Kim, H.M. Lee and D.H. Yoon, *Thin Solid Films* 475 (2005): 239.

[63] M. Tanaka, T. Suzuki and T. Nishinaga, *J. Cryst. Growth* 111 (1991): 168.

[64] M.F. Lovisa and G. Ehrlich, *Surf. Sci.* 246 (1991): 43.

[65] J.H. Neava, P.J. Dobson and B.A. Joyce, *Appl. Phys. Lett.* 47 (1985): 100.

[66] S. Das Sarma and P.I. Tamborenea, *Phys. Rev. Lett.* 66 (1991): 325.

[67] P.I. Tamborenea and S. Das Sarma, *Phys. Rev. E* 48 (1993): 2575.

[68] T. Karabacak and T.-M. Lu, *J. Appl. Phys.* 97 (2005): 124504.

Vitae

Chalasai Chaiyasorn was born on April 25, 1981 in Nakhon Si Thammarat, Thailand. He received Bachelor's Degree of Science in Physics from Chulalongkorn University in 2003.

CONFERENCE PRESENTATIONS:

2008 C. Chaiyasorn and P. Chatraphorn. Asymptotic Growth Exponent in a Ballistic Deposition Model for Thin Film Growth with Void Defect. Siam Physics Congress 2008, Nakhon Ratchasima, Thailand (20-22 March; 2008)

2007 C. Chaiyasorn and P. Chatraphorn. Ballistic Deposition Model with Two Different Interpretations of Surface Diffusion. Siam Physics Congress 2007, Nakhon Pathom, Thailand (22-24 March; 2007)

2006 C. Chaiyasorn and P. Chatraphorn. Patterned-Substrate Growth by Ballistic Deposition Model with Thermal Activation. 32nd Congress on Science and Technology of Thailand, Chulalongkorn University (10-12 October; 2006)

PUBLICATION:

2008 C. Chaiyasorn and P. Chatraphorn, Ballistic Deposition Model with Two Different Interpretations of Surface Diffusion, *Thai Journal of Physics* 3 (2008): 21.